OPTIMAL POWER FLOW INCLUDING VOLTAGE STABILITY

GNANAPRABHU GNANAM

INFORMATION TO USERS

This manuscript has been reproduced from the microfilm master. UMI films the text directly from the original or copy submitted. Thus, some thesis and dissertation copies are in typewriter face, while others may be from any type of computer printer.

The quality of this reproduction is dependent upon the quality of the copy submitted. Broken or indistinct print, colored or poor quality illustrations and photographs, print bleedthrough, substandard margins, and improper alignment can adversely affect reproduction.

In the unlikely event that the author did not send UMI a complete manuscript and there are missing pages, these will be noted. Also, if unauthorized copyright material had to be removed, a note will indicate the deletion.

Oversize materials (e.g., maps, drawings, charts) are reproduced by sectioning the original, beginning at the upper left-hand corner and continuing from left to right in equal sections with small overlaps. Each original is also photographed in one exposure and is included in reduced form at the back of the book.

Photographs included in the original manuscript have been reproduced xerographically in this copy. Higher quality 6" x 9" black and white photographic prints are available for any photographs or illustrations appearing in this copy for an additional charge. Contact UMI directly to order.

UMI

A Bell & Howell Information Company
300 North Zeeb Road, Ann Arbor MI 48106-1346 USA
313/761-4700 800/521-0600

OPTIMAL POWER FLOW INCLUDING VOLTAGE STABILITY

By

Gnanaprabhu Gnanam B.E.

A THESIS

SUBMITTED TO THE SCHOOL OF GRADUATE STUDIES

IN PARTIAL FULFILLMENT OF THE REQUIREMENTS

FOR THE DEGREE OF

MASTER OF ENGINEERING

FACULTY OF ENGINEERING AND APPLIED SCIENCE

MEMORIAL UNIVERSITY OF NEWFOUNDLAND

St. John's, Newfoundland, Canada

December 1996

Abstract

This thesis investigates the effects of including a voltage stability index as part of Security Constrained Optimal Power Flow (SCOPF). The formulation of Optimal Power Flow (OPF) and SCOPF, and their computational features are discussed. Different types of voltage stability indices are studied and an L-index based voltage stability index is used for the investigation. Two different approaches are used in formulating the L-index in SCOPF. In one method, the L-index was formulated as a part of SCOPF constraints. In the other, the L-index is used as the SCOPF objective function. The effects of these methods on the voltage stability of the system are determined by monitoring the voltage stability margin. Simulation results based on the two methods are presented for a 6-bus system and 30-bus system. The advantages and disadvantages of both the methods are discussed. Simulation results indicate that, the method with L-index as SCOPF objective function significantly improves the voltage stability margin compared to the standard SCOPF.

Acknowledgments

I would like to express my deep gratitude and thanks to my supervisor, Dr. Benjamin Jeyasurya, for his invaluable guidance and support during all stages of this work. I sincerely thank Dr. B. Jeyasurya, the School of Graduate Studies and the Faculty of Engineering and Applied Science for the financial support provided to me during the course of my M.Eng. program.

I sincerely thank Dr. J. J. Sharp, Associate Dean for Graduate Studies for his encouragement and support during my study in Canada. In addition, I would like to thank the faculty members, fellow graduate students and other staffs of the Faculty of Engineering and Applied Science for their help and assistance.

Finally, I would like to dedicate this thesis to my parents. Words cannot express my gratitude for all that they have done.

Contents

Abstract

Acknowledgments i

Table of Contents ii

List of Figures ii

List of Tables iii

List of Symbols iv

1 Introduction 1

1.1 Introduction 1

1.2 Power System Optimization and Voltage Stability 2

1.2.1 Optimal Power Flow 2

1.2.2 Voltage Stability 3

1.3 Aim of the thesis 4

1.4 Organization of the thesis 6

2 Optimal Power Flow 7

2.1 Introduction 7

2.2 Optimal Power Flow Formulation 7
2.2.1 Control variables 8
2.2.2 State variables 9
2.2.3 Objective Function 9
2.2.4 Equality constraints 11
2.2.5 Inequality constraints 12
2.3 Classification of Optimal Power Flow 14
2.3.1 Class A 14
2.3.2 Class B 15
2.4 Optimization Methodology 15
2.4.1 Description of MINOS 16
2.4.2 Optimal Power Flow Program 18
2.5 Simulation Results 18
2.5.1 The 6-Bus System 18
2.5.2 14-Bus System 19
2.5.3 IEEE 30-Bus System 21
2.6 Summary 23

3 Security Constrained Optimal Power Flow 25
3.1 Introduction 25
3.2 Security Concepts 25
3.3 Advantages of SCOPF 27
3.4 Types of Security Constrained Optimal Power Flow 29
3.4.1 The Non-decomposed approach 29
3.4.2 The Decomposed approach 29
3.4.3 Formulation of Security Constraint Optimal Power Flow . . . 30

3.5 Computational Aspects 31
3.6 Simulation Results 32
3.7 Summary 36

4 Voltage Stability **38**

4.1 Introduction 38
4.2 Definitions 38
4.3 Mechanism of Voltage Collapse 39
4.4 Static vs Dynamic Analysis 41
4.5 Methods of Voltage Stability Analysis 41
4.5.1 P-V curves 41
4.5.2 V-Q curves 43
4.6 Continuation Power Flow 45
4.6.1 Prediction 47
4.6.2 Parameterization and Corrector 48
4.7 Minimum Singular Value method 50
4.8 Kessel and Glavitch method 52
4.9 Summary 54

5 Optimal Power Flow including Voltage Stability **56**

5.1 Introduction 56
5.2 Optimal Power Flow including Voltage Stability Index 56
5.3 Voltage Stability Margin Enhancement 58
5.3.1 L-index as OPF constraints 58
5.3.2 L-index as OPF objective 61
5.4 Simulation Results 62

5.4.1 6-Bus system 64
5.4.2 30-Bus system 68
5.5 Summary 72

6 Conclusions **73**
6.1 Contributions of the Research 73
6.2 Future Work 74

References **76**

Appendices **81**

A Optimal Power Flow Program **81**
A.1 Main Module 81
A.2 Line data file 81
A.3 Bus data file 82
A.4 Generator data file 83
A.5 Problem definition file 84
A.6 Sample data files 85
A.7 Optimization process 85
A.8 Running the OPF problem 85
A.9 Output file 86
A.10 Example 87

B OPF System Data **94**

List of Figures

2.1 The 6-bus system 18

2.2 14 bus system 20

2.3 IEEE 30 bus system 22

3.1 Power system static security levels 26

3.2 Two bus system 28

3.3 OPF solution 28

3.4 SCOPF solution 29

3.5 OPF solution for 6-bus system 32

3.6 Contingency load flow for 6-bus system (for opf) 33

3.7 SCOPF solution for 6-bus system 34

3.8 Contingency load flow for 6-bus system (for SCOPF) 34

3.9 Modified IEEE 30-Bus system. 35

4.1 Radial system used to demonstrate the voltage collapse mechanism . 39

4.2 P-V curves 43

4.3 V-Q curves 44

4.4 Continuation Power Flow 45

4.5 Continuation Power Flow for the 6-bus system 50

4.6 Continuation Power Flow for the 30-bus system 50

4.7 Minimum Singular Value for the 6-bus system 52
4.8 Minimum Singular Value for the 30-bus system 52
4.9 L-index for the 6-bus system 54
4.10 L-index for the 30-bus system 54

5.1 Continuation Power Flow for the base case and a line outage case for the 6 bus system 59
5.2 Continuation Power Flow for the base case and a line outage case for the 30 bus system 59
5.3 P-V curves (CPF method) for the 6 bus system 67
5.4 P-V curves (CPF method) for the 30 bus system 71

List of Tables

2.1 OPF results for the 6-Bus system 19

2.2 OPF results for the 14-Bus system 21

2.3 OPF results for the IEEE 30-Bus system 23

3.1 SCOPF results for the 6-Bus system 35

3.2 SCOPF results for the IEEE 30-Bus system 36

4.1 CPF for the 6-bus system 49

5.1 OPF with L-index for the 6-Bus system 64

5.2 OPF with L-index (L_{max}=0.75) for the 6-Bus system 65

5.3 OPF with L-index as objective function for the 6-Bus system 66

5.4 Comparison of OPF results with voltage stability index for 6-Bus system 67

5.5 OPF with L-index for the 30-Bus system 68

5.6 OPF with L-index (L_{max}=0.8000) for the 30-Bus system 69

5.7 OPF with L-index as objective function for the 30-Bus system 70

5.8 Comparison of OPF results with voltage stability index for 30-Bus system 72

A.1 OPF input data files for various test systems 85

B.1 Line data for the 6-Bus system 94
B.2 Bus data for the 6-Bus system 95
B.3 Generator data for the 6-Bus system 95
B.4 Line data for the IEEE-14 Bus system 95
B.5 Bus data for the IEEE-14 Bus system 96
B.6 Generator data for the IEEE-14 Bus system 96
B.7 Line data for the 30-Bus system 97
B.8 Bus data for the 30-Bus system 98
B.9 Generator data for the 30-Bus system 98

List of symbols

The following is a list of the most extensively used symbols and notations in this thesis.

$\|u\|$: *vector of control variables.*

$\|x\|$: *vector of state variables.*

$f(u,x)$: *objective function.*

$g(u,x)$: *set of equality constraints.*

$h(u,x)$: *set of inequality constraints.*

$\alpha_i, \beta_i, \gamma_i$: *the fuel cost coefficient of the generator at bus i*

P_i : *active power injection at bus i.*

Q_i : *reacive power injection at bus i.*

P_{G_i} : *real power generation at bus i.*

Q_{G_i} : *reactive power generation at bus i.*

P_{D_i} : *real power load at bus i.*

Q_{D_i} : *reactive power load at bus i.*

δ_i : *angle at bus i with respect to the refence bus.*

V_i : *voltage magnitude of bus i.*

t_{ij} : *tranformer tap settings between bus i and j.*

P_{ij} : *active power flow in the line ij.*

Q_{ij} : *reactive power flow in the line ij.*

S_{ij} : *apparent power flow in the line ij.*

I_{ij} : *current flow in the line ij.*

R_{ij} : *resistance of line ij.*

X_{ij} : *reactance of the line ij.*

s_i : *shunt capacitance at bus i*

t_{ij} : *tap settings of the transformer located between bus i and j*

L_i : *value of $L-$index at bus i.*

Chapter 1

Introduction

1.1 Introduction

An important requirement of the modern civilization is the economic and secure operation of its electric power system. The Energy Management System (EMS) plays an important role in the power industry to meet this challenge. Optimal Power Flow (OPF) is an integral part of any modern EMS which helps to maintain the economy of the power system. At present, on-line OPF is the most complex application in the EMS. In the area of system planning, OPF is used for capacitor placement studies and transmission capacity planning. Very recently Security Constrained Optimal Power Flow (SCOPF) are used in the EMS to achieve the combined goal of ecomony and security of the power system. In the recent years, full utilization of transmission lines for economic reasons has increased the vulnerability of the power system networks. Many electric utilities have reported events related to voltage stability with losses in millions of dollars. This chapter presents the aim of this thesis and an overview of Optimal Power Flow and Voltage Stability. This chapter also presents the organization of this thesis.

1.2 Power System Optimization and Voltage Stability

This section gives an overview of Optimal Power Flow and Voltage Stability, and a review of research on the topic in recent years.

1.2.1 Optimal Power Flow

Optimal Power Flow is a power flow problem which gives the optimal settings of the control variables for given settings of load by minimizing a selected objective function such as the cost of active power generation or losses. OPF also considers the operating limits of the system. Following the "classical" OPF formulation by Dommel and Tinney [1], a number of different methods have been presented to solve the OPF problem. Some of the recent review papers [2, 3] give a comprehensive picture of the state-of-the-art over the past 30 years. Dommel and Tinney [1] proposed a method based on the ordinary load flow solution which uses a reduced gradient algorithm to obtain the optimal solution. This method uses a penalty function to account for the dependent constraints. The main disadvantage of this method lies in handling the constraints using penalty functions and the convergence of the approach was poor.

One of the important aspects of the system is the steady-state security. This is defined as the ability of the system to operate within the system operating limits and maintain the supply following a contingency. Security Constrained Optimal Power Flow (SCOPF) is an OPF which takes into account the steady state security of the system. In the early seventies Alsac and Stott [4] proposed a non-decomposed approach to solve contingency-constrained OPF problem. The approach involved the formulation of a single large OPF problem which includes the constraints for all

the severe contingencies in the system. The main disadvantage of this method is that the problem size increases with the number of contingencies. Another traditional approach to solve the SCOPF problem is the decomposed approach [5], in which the base case problem is augmented with a small number of post contingency violating constraints, and the problem is solved iteratively till no violation occurs in the post contingency state.

Reference [6] proposed an optimal corrective rescheduling algorithm to maintain the power system security. In this method the post contingency violations in the system are corrected by rescheduling the generation and power interchange in an optimal way. Reference [7] gives a decoupled global VAR dispatch method by formulating the contingency constraints as a part of the optimal reactive power dispatch problem. Modeling the system parameters plays an important role in maintaining the security. The effect of load modeling in SCOPF are studied in [8]. The influence of fixed tap transformer fed loads in SCOPF is studied in [9].

1.2.2 Voltage Stability

Voltage stability problem has received increasing attention over the past few years. Several occurrence of voltage stability problem all over the world [10, 11] have been reported. Reference [12] shows that each of the events occurred for various reasons. Voltage collapse is associated to a saddle node bifurcation point [13, 14]. For a particular loading condition more than one solutions exist for a load flow solution, out of which one solution is the actual operating point. The other solutions are related to the unstable equilibrium point (u.e.p). For any given pattern of load increase these equlibirium points approach each other and at one particular point there exists only one solution. This point is associated with the saddle node equilibrium point of the

voltage collapse point. Not all voltage collapse problems are caused by bifurcation phenomena. Some voltage collapse problems may be caused by fast dynamic events that are no way related to the bifurcation phenomena.

At the bifurcation point, the real eigenvalue of the load flow Jacobian becomes singular. Voltage collapse indices based on singular value and eigenvalue are discussed in [15] and [16]. In [17] the author has proposed a voltage stability index based on a test function. This index seems to have a linear behavior as the system approaches the point of collapse and gives a better idea how close the system is with respect to the point of collapse. In reference [18] the authors have proposed a voltage stability proximity index based on the voltage phasor values at a given operating point. However, this method has a difficulty in identifying the "right" transmission path to monitor the voltage proximity index which changes when the system operating limits are considered. Reference [19] has successfully employed an Energy Function method to evaluate the voltage stability condition.

1.3 Aim of the thesis

Optimal Power Flow plays an important role in maintaining the economy of the power system. Very recently, Security constrained Optimal Power Flow programs are used in the EMS to maintain the combined goal of economic secure operation of the power utilities. However, due to the sharp increase in the power demand over the past few years, utilities are forced to operate very close to the system limits. The electric power system operating under this condition has experienced serious stability problems. Stability problems related to voltage stability has been a major issue over the past few years. Researchers are focusing their attention to improve the voltage stability of the system. Recently optimal power flow has been

used in the shunt reactive power (VAR) support to improve the voltage stability of the system [20]. An optimal reactive power planning algorithm in connection with the continuation power flow algorithm is used to minimize the amount of shunt VAR support at the buses that are susceptible to voltage collapse. Reference [21] presents a method to determine the VAR supply to maintain the voltage profile and to maintain a safe stability margin with respect to the voltage stability.

Reference [22] has proposed a method for remedial action in a stressed power system. Remedial action uses a linear programming algorithm to remove the violations in the operating constraints with an objective to minimize the action of control variables. The remedial actions have always led to an improvement in the voltage stability of the system even though voltage stability enhancement was not an explicit objective.

The investigation carried out in this research includes explicit voltage stability constraints in optimal power flow to enhance the voltage stability margins. This will enable the power system to be operated in a cost effective manner. In addition, it will be possible to operate the system in a secure manner (ie. the power system will be secure against possible over loadings.

The objectives of this thesis are:

- to evaluate the Security Constrained Optimal Power Flow (SCOPF) used to maintain the security and economy in the power system.
- to investigate voltage stability analysis and evaluate some voltage stability indices used to determine the proximity of voltage instability in the system.
- to investigate the effects of including a suitable voltage stability index as part of Security Constrained Optimal Power Flow.

1.4 Organization of the thesis

This thesis is divided into six chapters. Chapter 1 is the introductory chapter. Chapter 2 presents the Optimal Power Flow (OPF) problem and simulation results on test power systems. Chapter 3 presents the Security Constrained Optimal Power Flow (SCOPF) and the advantages of SCOPF over OPF. Chapter 3 also presents the simulation results of the SCOPF on the test power systems. Chapter 4 discusses the voltage stability and the different methods to evaluate the proximity to voltage collapse in a power system. Three such methods are discussed in detail and simulation results on the test power systems are provided. Chapter 5 proposes a technique to include the voltage stability index as a part of Optimal Power Flow and the significance of this method is discussed. Simulation results based on this new method are also provided for the test power systems. Chapter 6 concludes the thesis and outlines some suggestions for future research.

Chapter 2

Optimal Power Flow

2.1 Introduction

Optimal Power Flow (OPF) plays an important role in power system operations and planning. In the normal operating condition OPF is used to determine the load flow solution which satisfies the system operating limits and minimize the generation costs. In power system planning, OPF is used for capacitor placement studies and transmission capability studies. This chapter discusses the formulation of the Optimal Power Flow problem in detail. The OPF simulation results are presented for three sample test systems, namely a 6-Bus system, IEEE 14-Bus system and IEEE 30-Bus system.

2.2 Optimal Power Flow Formulation

Optimal Power Flow (OPF) is a power flow problem which gives the optimal settings of the control variables for a given settings of load by minimizing a selected objective function such as the cost of active power generation or losses. OPF also considers the operating limits of the system. Following the "classical" OPF formulation by Dommel and Tinney [1], a number of different methods have been presented to solve the OPF problem. In general, OPF is formulated as a constrained optimization

problem as

$$Minimize \quad f(u,x) \tag{2.1}$$

$$Subject\ to \quad g(u,x) = 0 \tag{2.2}$$

$$h(u,x) \leq 0 \tag{2.3}$$

where

$\|u\|$: *vector of control variables.*

$\|x\|$: *vector of state variables.*

$f(u,x)$: *Objective function.*

$g(u,x)$: *set of equality constraints.*

$h(u,x)$: *set of inequality constraints.*

2.2.1 Control variables

These are the set of variables which can be modified to satisfy the load-flow equations. The set of control variables in OPF are:

- Active power generation of a Voltage controlled bus.
- Voltage magnitude of a Voltage controlled bus.
- Tap settings of a transformer.
- Shunt capacitance or reactance.

2.2.2 State variables

These are the set of variables which describe any unique state of the system. The set of state variables for the power system load flow problem are

- Voltage magnitude of all the buses.
- Voltage angle of all the buses.

2.2.3 Objective Function

The objectives commonly used in power system optimization are as follows:

- *Minimize the cost of operations* : This objective is used to minimize the total generation cost in the system. Usually the operation cost of the thermal units in the system are minimized. The cost for the thermal units are derived from the heat rate curves (cost versus MW) and expressed as a convex polynomial or exponential term. The sum of all such terms for the thermal units are minimized.
- *Minimize the real power losses* : The sum of the losses of all brances in the system are minimized. This results in the reduction of active power generation in the system, which saves both the generation cost and creates a higher generation reserves.
- *Minimize the reactive power losses* : This objective function minimizes the amount of reactive power (VAr) support which indirectly minimizes the reactive power losses in the system. This results in a better voltage profile in the system.

- *Maximize the MW transfers* : This objective used to maximize the power transfer within a given system which indirectly minimizes the amount of reactive power support in the system. This objective is used to detemine the maximum tranfer limits in the system.

- *Minimize the cost of installation of new capacitors and reactors* : This objective is usually used in the system planning studies to allocate more reactive power support to the system. This objective minimizes the total cost involved in installing new capacitors and reactors to meet the required reactive power support.

- *Minimize the number and deviation in control variables* : This objective is usually defined as the sum of deviation of the weighted squires of the deviations of the control variables from their current operating point. This objective is used when it is impossible to reschedule a large number of control at the same time.

In the OPF formulation presented in this thesis, two objectives are considered, (i) to minimize the cost of operation and (ii) to minimize the real power losses in the system. All the generator units in the system are assumed to be thermal units. The cost functions are expressed as a quadratic function of the real power generations. The objective functions used to minimize the total system operating cost can be described as

$$Minimize \quad \sum_{i=1}^{N_g} \alpha_i + \beta_i P_{Gi} + \gamma_i P_{Gi}^2 \tag{2.4}$$

where

N_g : *number of generators in the system*

$\alpha_i, \beta_i, \gamma_i$: *the fuel cost coefficient of the generator at bus i.*

P_{Gi} : *real power generation at bus i.*

The objective function used to minimize the real power loss in the system can be described as follows:

$$Minimize \quad \sum_{i=1}^{m} G_{ij}(V_i^2 + V_j^2 - 2V_iV_j\cos\delta_{ij}) \tag{2.5}$$

where

m : *number of lines in the system*

G_{ij} : *transfer conductance of the line ij.*

Note that each term in the summation gives the real power loss in a transmission line.

2.2.4 Equality constraints

The equality constraints are the load-flow equations. For each bus in a power system, there are two equations:

- Real power balance equation.

$$P_{G_i} - P_{D_i} - P_i(V, \delta, t) = 0 \tag{2.6}$$

- Reactive power balance equation.

$$Q_{G_i} - P_{D_i} - Q_i(V, \delta, t) = 0 \tag{2.7}$$

$$P_i = \sum V_i V_j [G_{ij} \cos(\delta_i - \delta_j) + B_{ij} \sin(\delta_i - \delta_j)] \tag{2.8}$$

$$Q_i = \sum V_i V_j [B_{ij} \cos(\delta_i - \delta_j) - G_{ij} \sin(\delta_i - \delta_j)] \tag{2.9}$$

where

P_i : *active power injection at bus i.*

Q_i : *reacive power injection at bus i.*

P_{G_i} : *real power generation at bus i.*

Q_{G_i} : *reactive power generation at bus i.*

P_{D_i} : *real power load at bus i.*

Q_{D_i} : *reactive power load at bus i.*

G_{ij} : *real part of ybus element ij*

B_{ij} : *imaginary part of ybus element ij.*

δ_i : *angle at bus i with respect to the refence bus.*

V_i : *Voltage magnitude of bus i.*

t_{ij} : *tranformer tap settings between bus i and j.*

2.2.5 Inequality constraints

The inequality constraints are the system operating limits. The inequality constraints are [8]

- Limits of the real and reactive power generation at the Generator buses.

$$P_{G_{low_i}} \leq P_{G_i} \leq P_{G_{high_i}} \tag{2.10}$$

$$Q_{G_{low_i}} \leq Q_{G_i} \leq Q_{G_{high_i}} \tag{2.11}$$

- Limits of Voltage magnitude and angle at all the buses.

$$\|V\|_{low_i} \leq \|V_i\| \leq \|V_{high_i}\| \tag{2.12}$$

$$\theta_{low_i} \leq \theta \leq \theta_{high_i} \tag{2.13}$$

- Limits on the tap setting of the transformers.

$$t_{low_{ij}} \leq t_{ij} \leq t_{high_{ij}} \tag{2.14}$$

- Limits on the shunt capacitance and reactances.

$$s_{low_i} \leq s_i \leq s_{high_i} \tag{2.15}$$

- Limits on the power flow in transmission, apparent power flow in the transmission line and current flows in the lines.

$$P_{ij} \leq P_{high_{ij}} \tag{2.16}$$

$$P_{ij}^2 + Q_{ij}^2 \leq S_{high_{ij}}^2 \tag{2.17}$$

$$\|I\|_{ij} \leq \|I\|_{high_{ij}} \tag{2.18}$$

The variables in equations 2.16 to 2.18 are defined as [8]

$$\begin{aligned} P_{ij} &= \frac{1}{t_{ij}[R_{ij}^2 + X_{ij}^2]}[-R_{ij}V_iV_j\cos(\theta_i - \theta_j) \\ &\quad + X_{ij}V_iV_j\sin(\theta_i - \theta_j) + V_i^2 R_{ij}\frac{1}{t_{ij}}] \end{aligned} \tag{2.19}$$

$$Q_{ij} = \frac{1}{t_{ij}[R_{ij}^2 + X_{ij}^2]}[-X_{ij}V_iV_j\cos(\theta_i - \theta_j) - R_{ij}V_iV_j\sin(\theta_i - \theta_j) + V_i^2 X_{ij}\frac{1}{t_{ij}}] \quad (2.20)$$

$$I_{ij}^2 = \frac{S_{ij}^2}{V_i^2} \quad (2.21)$$

$$S_{ij}^2 = P_{ij}^2 + Q_{ij}^2 \quad (2.22)$$

where

P_{ij} : *active power flow in the line ij.*

Q_{ij} : *reactive power flow in the line ij.*

S_{ij} : *apparent power flow in the line ij.*

I_{ij} : *current flow in the line ij.*

R_{ij} : *resistance of line ij.*

X_{ij} : *reactance of the line ij.*

s_i : *shunt capacitance at bus i*

t_{ij} : *tap settings of the transformer located between bus i and j*

2.3 Classification of Optimal Power Flow

The OPF methods are commonly classified into two types:

2.3.1 Class A

In this method the OPF starts from a solved load flow solution. The Jacobian and other sensitivity relations are used in the optimization process. This involves

iterative process which calculates the load flow solution in every iteration. An example for this method is the method by Dommel and Tinney [1]. This method uses the power flow solution as the starting point and a gradient method is used to obtain the optimal point. The basic idea is to move from one feasible solution point to another in the direction of steepest descent.

2.3.2 Class B

This method uses the exact optimality conditions where the load flow equations are formulated as equality constraints. There is no need of a load flow solution. Most of these methods are based on the Kuhn-Tucker optimality conditions [23]. The Kuhn-Tucker condition determines whether at any given solution point a relative optimum has been reached. The inequality constraints on variables and functions are enforced by penalty functions. It should be noted that there are no unique penalty based approaches known today for solving the Kuhn-Tucker conditions with straight forward solution processes. To improve speed and convergence, heuristic methods are used which involve many trial iterations and soft limit enforcements. The main advantage of this method lies in the fact that the Hessian matrix, which is a symmetric matrix of second partial derivative of the power flow equations with respect to the state variables is sparse and remains constant. The Newton based OPF method proposed by Sun et.al. [24] falls in this category.

2.4 Optimization Methodology

The OPF problem was solved using MINOS version 5.4 [25]. MINOS is one of the most popular general purpose optimization tools used to solve the OPF problem. MINOS is capable of solving optimization problems with nonlinear objective and

nonlinear constraints.

2.4.1 Description of MINOS

MINOS is coded in FORTRAN, which is designed to be almost machine-independent and to operate primarily within main memory. MINOS is based on the Wolfe's reduced-gradient algorithm [26]. The nonlinear constrained optimization problem can be expressed as

$$Minimize \quad f^0(x) + c^T x + d^T y \tag{2.23}$$

$$Subject\ to \quad f(x) + A_1 y = b_1 \quad (m_1 \ \ rows) \tag{2.24}$$

$$A_2 x + A_3 y = b_2 \quad (m_2 \ \ rows) \tag{2.25}$$

$$l \leq \begin{bmatrix} x \\ y \end{bmatrix} \leq u \quad m = m_1 + m_2 \tag{2.26}$$

where $f(x) = [f^1(x), ..., f^{m_1}]^T$. The variable x is a 'non-linear variable' and the variables y is a linear variables.

The solution process involves a sequence of major iterations, which requires the linearization of the nonlinear constraints at each point of x_k corresponding to the first order Taylor's series approximation. At each major iteration the linearized subproblem is given by

$$Minimize_{x,y} \quad L(x, y, x_k, \lambda_k, \rho) = f^0(x) + c^T x + d^T y - \lambda_k^T (f - \tilde{f})$$
$$+ \frac{1}{2}\rho(f - \tilde{f})^T (f - \tilde{f}) \tag{2.27}$$

$$Subject\ to \quad \tilde{f} + A_1 y = b_1 \tag{2.28}$$

$$A_2 x + A_3 y = b_2 \tag{2.29}$$

$$l \leq \begin{bmatrix} x \\ y \end{bmatrix} \leq u \tag{2.30}$$

$$f - \bar{f} = (f - f_k) - J_k(x - x_k) \tag{2.31}$$

where $J(x)$ is the Jacobian matrix, λ_k is the vector of lagrangian multipliers and ρ is the penalty parameter.

The variables in the linearized subproblem are partitioned as [B S N], where B is the basic variables, S is the super basic variables and N represents the non-basic variables. The active constraints can be written as

$$\begin{bmatrix} BSN \\ I \end{bmatrix} \begin{bmatrix} x_B \\ x_S \\ x_N \end{bmatrix} = \begin{bmatrix} b \\ n_N \end{bmatrix} \tag{2.32}$$

In the active constraint matrix $A = \begin{bmatrix} BSN \\ I \end{bmatrix}$, the last few coulmns represent the identity matrix I. Consider an operator Z which satisfies the condition AZ=0 such that $Z = \begin{bmatrix} -B^{-1} \\ I \\ 0 \end{bmatrix}$

The feasible desent direction D^k can be obtained using

$$Z^T G Z D_s^k = -Z^T g \tag{2.33}$$

$$D^k = Z D_s^k \tag{2.34}$$

where g is the gradient of the objective function.

A quasi-Newton approach is used to find the search direction D_s^k, by replacing the Hessian with a positive definitive approximation.

Now the value of X^k is updated to $X^k + \alpha^k D^k$. The scalar α^k is obtained by using a line search such that it will lower the value of the objective function. This processes is repeated till an optimal point is reached.

2.4.2 Optimal Power Flow Program

This section describes the OPF program which was developed to solve the OPF problem using MINOS. The program was written in C++ [27]. This program reads the system data from four different files which are used to solve the OPF problem. The details of these files are given in Appendix A. This program formulates the OPF problem in standard files as required by MINOS to solve the optimization problem. The details of the standard input file required by MINOS are given in [25]. MINOS independently solves the OPF problem and the results are stored in the output file. All these programs are developed in a UNIX environment.

2.5 Simulation Results

2.5.1 The 6-Bus System

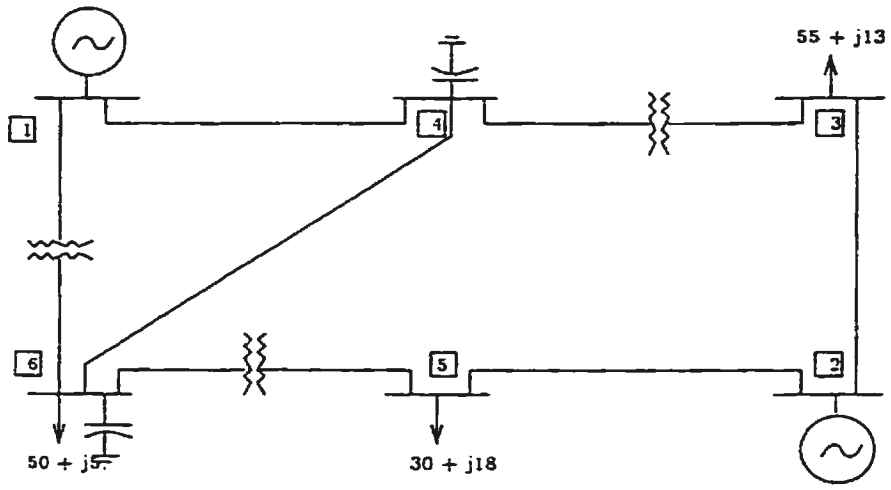

Figure 2.1: The 6-bus system

Figure 2.1 shows the 6-bus system which has 7 lines, 2 generators, 3 tap-changing transformers and 2 capacitors. The bus data and generator data for the system are given in Appendix B. The lower voltage magnitude limits for all the buses are 0.95

p.u. The upper limits are 1.1 p.u for the generator buses 1,2 and 1.05 p.u for all the load buses. The results of the OPF with minimum cost and loss objectives along with the base case load flow solution are summarized in Table 2.1. The 'Base case' refers to the load flow solution without any optimization objective. The OPF with cost objective function results in a total operating cost of 601.25 $/hr and total system loss of 8.078 MW. The OPF with minimum loss objective function results in a total operating cost of 813.76 $/hr and a total system loss of 6.241 MW. It can be seen that the total operating cost of the system is considerably high while minimizing the total losses in the system. For simplicity only the value of the control variables are shown in the table.

Table 2.1: OPF results for the 6-Bus system

Control variables	Base case	Min. Cost	Min. Loss
V_1 (p.u)	1.1	1.1	1.1
V_2 (p.u)	1.1	1.1	1.1
P_{G_2} (MW)	50.0	50.0	26.45
Q_{c_4} (Mvar)	14.4	12.54	13.24
Q_{c_6} (Mvar)	15.6	17.50	17.50
T_1	0.991	0.9657	0.9500
T_2	0.944	0.9847	0.9543
T_3	1.013	0.9810	1.0153
Operating cost [$/hr]	604.58	601.25	813.76
Loss [MW]	8.40	8.078	6.241

2.5.2 14-Bus System

Figure 2.2 shows the IEEE 14-bus system which has 20 lines, 5 generators, 3 tap-changing transformers. The bus data and generator data for the system are given in

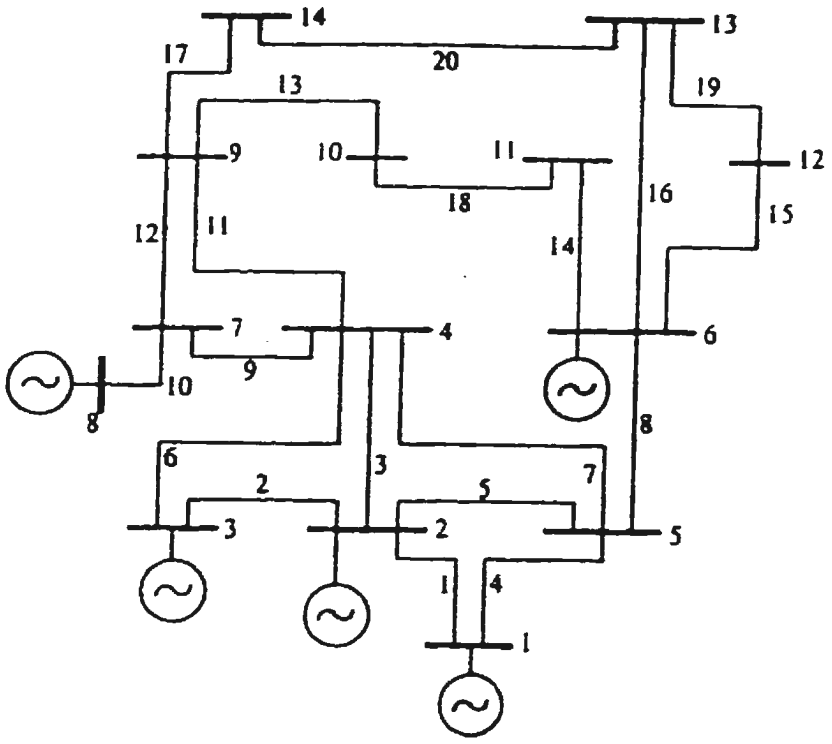

Figure 2.2: 14 bus system

Appendix B. The voltage magnitude limits for all the load buses are between 0.95 and 1.05 p.u. The voltage magnitude limits for all the generator buses are between 0.95 and 1.1 p.u.

The tap-changing transformers are allowed to vary between the range 0.9 to 1.1. The results of the OPF with the two different objective functions and the base case load flow solution are summarized in Table 2.2. The OPF with cost objective results in a total cost of 1043 $/hr and loss of 5.124 MW. The OPF with minimimum loss objective results in a total operating cost of 1344.86 $/hr and loss of 1.648 MW.

Table 2.2: OPF results for the 14-Bus system

Control variables	Base case	Min. Cost	Min. Loss
V_1 (p.u)	1.0500	1.0500	1.0500
V_2 (p.u)	1.0450	1.0393	1.0500
V_3 (p.u)	1.0300	1.0295	1.0434
V_6 (p.u)	1.0500	1.0500	1.0500
V_8 (p.u)	1.0500	1.0500	1.0500
P_{G_2} (MW)	34.0	28.71	58.71
P_{G_3} (MW)	80.0	80.00	80.00
P_{G_6} (MW)	50.0	34.45	88.13
P_{G_8} (MW)	50.0	33.78	70.00
$Q_{c_{10}}$ (Mvar)	10.0	11.84	11.74
Q_{c-11} (Mvar)	10.0	10.57	10.99
$Q_{c_{13}}$ (Mvar)	10.0	9.16	9.37
Q_{c-14} (Mvar)	10.0	5.20	5.20
T_1	1.0000	0.9884	1.0321
T_2	1.0000	1.1000	1.1000
T_3	1.0000	1.0185	1.0135
Operating cost [$/hr]	1075.58	1043.19	1344.86
Loss [MW]	4.309	5.124	1.648

2.5.3 IEEE 30-Bus System

Figure 2.3 shows an adaptation of the IEEE 30 bus system standard load-flow test system [4] with 41 lines, 6 generators, 4 tap-changing transformers and 2 fixed capacitors. The line data, generator data and load data for the system are given in the Appendix B. The lower voltage magnitude of all the buses are 0.95 p.u and the upper limits are 1.1 p.u for all the generator buses 2,5,8,11, and 13, and 1.05 p.u for all the remaining buses including the reference bus 1. The tap changing transformers

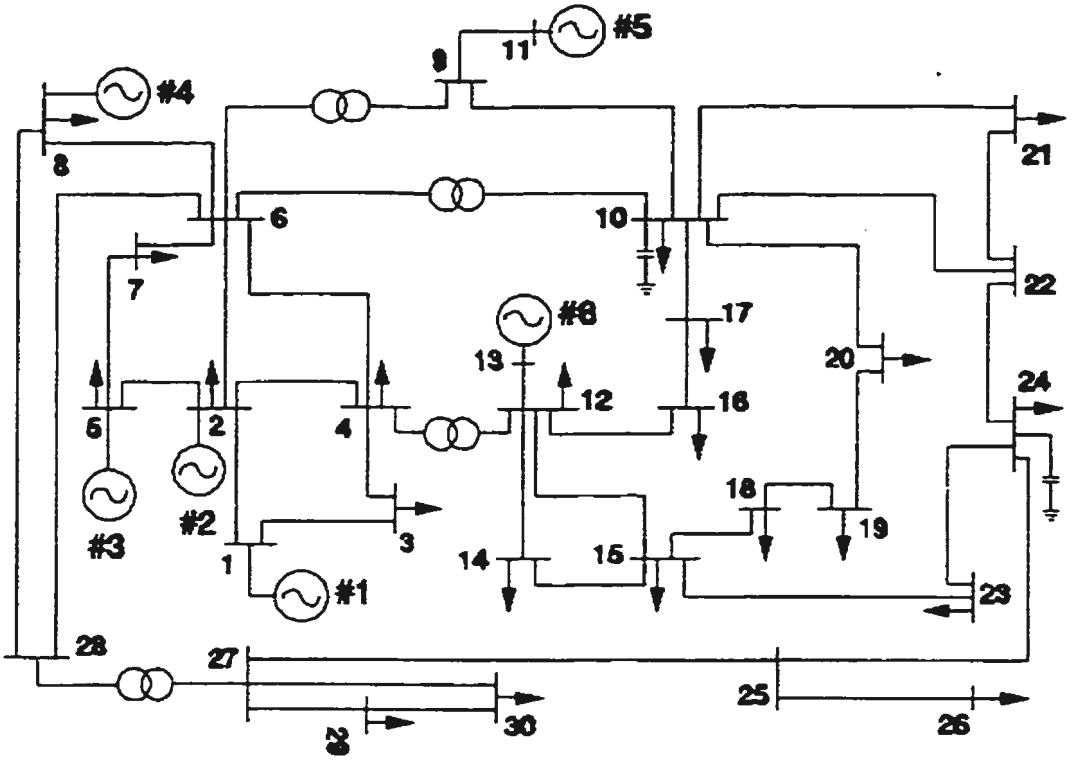

Figure 2.3: IEEE 30 bus system

are allowed to vary in the range between 0.9 and 1.1. The OPF results along with the base case solution are illustrated in Table 2.3.The OPF with minimizing the operating cost results with a total operating cost of 800.79 $/hr and loss of 8.646 MW. The OPF with minimum loss objective results with an operating cost of 967.82 $/hr and loss of 3.243 MW.

Table 2.3: OPF results for the IEEE 30-Bus system

Control variables	Base case	Min. Cost	Min. Loss
V_1 (p.u)	1.0500	1.0500	1.0500
V_2 (p.u)	1.0450	1.0381	1.0477
V_5 (p.u)	1.0100	1.0114	1.0294
V_8 (p.u)	1.0100	1.0191	1.0364
V_{11} (p.u)	1.0500	1.0891	1.0796
V_{13} (p.u)	1.0500	1.0858	1.0738
P_{G_2} (MW)	80.00	48.56	80.00
P_{G_5} (MW)	50.00	21.43	50.00
P_{G_8} (MW)	20.00	21.70	35.00
$P_{G_{11}}$ (MW)	20.00	12.06	30.00
$P_{G_{13}}$ (MW)	20.00	12.00	40.00
T_1	0.9780	1.0018	1.0031
T_2	0.9690	1.0468	1.0178
T_3	0.9320	1.0011	0.9972
T_4	0.9680	0.9425	0.9563
Operating cost [$/hr]	903.3	800.79	967.82
Loss [MW]	6.502	8.646	3.243

2.6 Summary

This chapter has discussed the formulation of Optimal Power Flow problem in detail. An Optimal Power Flow program was developed by using a general purpose optimization software MINOS which is capable of solving the sample test systems used in studying power systems. The OPF program is capable of handling two different objectives to minimize the total operating cost and to minimize the total system losses. Simulation results for the OPF using these two different objective functions were carried out on the 6-bus system. IEEE 14-bus system and the IEEE 30-bus

system. The results clearly shows that the OPF is better compared to the load flow solution, in terms of system operating cost and minimizing the losses. If the OPF with cost objective is implemented as a part of Energy Management System (EMS) the utility will save a substantial amount of money every year. Minimizing the MW losses in the system results in reducing the MVAR losses in the system. Loss minimization in the system will also result in substantial savings for the utility as the amount of total generation decreases and the total MVAR support required to operate the system is less. The choice of the objective function for the OPF depends on the needs of the utilities.

Chapter 3

Security Constrained Optimal Power Flow

3.1 Introduction

Chapter 2 has discussed the significance of optimal power flow in the power system operation. OPF helps to maintain the economic operation of the power system. Another important aspect of the power system is the steady-state security. This is defined as the ability of the power system to operate within its system limits following a contingency. Security Constrained Optimal Power Flow (SCOPF) is an extension of OPF which helps to maintain the combined goal of economy and security of the power system. This chapter introduces the concept of Power System Security and the formulation of SCOPF is discussed. The advantages of SCOPF compared to the OPF are highlighted with the example of simulation results for the test power systems. Simulation results are provided for a 6 bus system and a 30 bus system.

3.2 Security Concepts

The main aim of the power system security analysis is to design appropriate control measures to prevent the system from blackout. The operation of a power system

can be classified into four main states [30]. *Normal state* is one where all the loads are supplied and no equipment in the system is overloaded. The system is said to be secure and it can withstand a contingency without violating any constraints in the system. *Alert state* is a state where the system is operating within its limits but a contingency may violate some of the system limits. Following the *alert state* the system enters the *in extremis*, when a severe contingency occurs in the *alert state*. If the system continues to remain in this state, it results in cascading outages may occur and the system may lose a portion of the load. In this case a load shedding is initiated to prevent the system from a total blackout. The *restorative state* is one which takes the system from the *extrmis* to the *alert state* or *normal state*.

Reference [3] classifies power system security into six levels as shown in Figure 3.1.

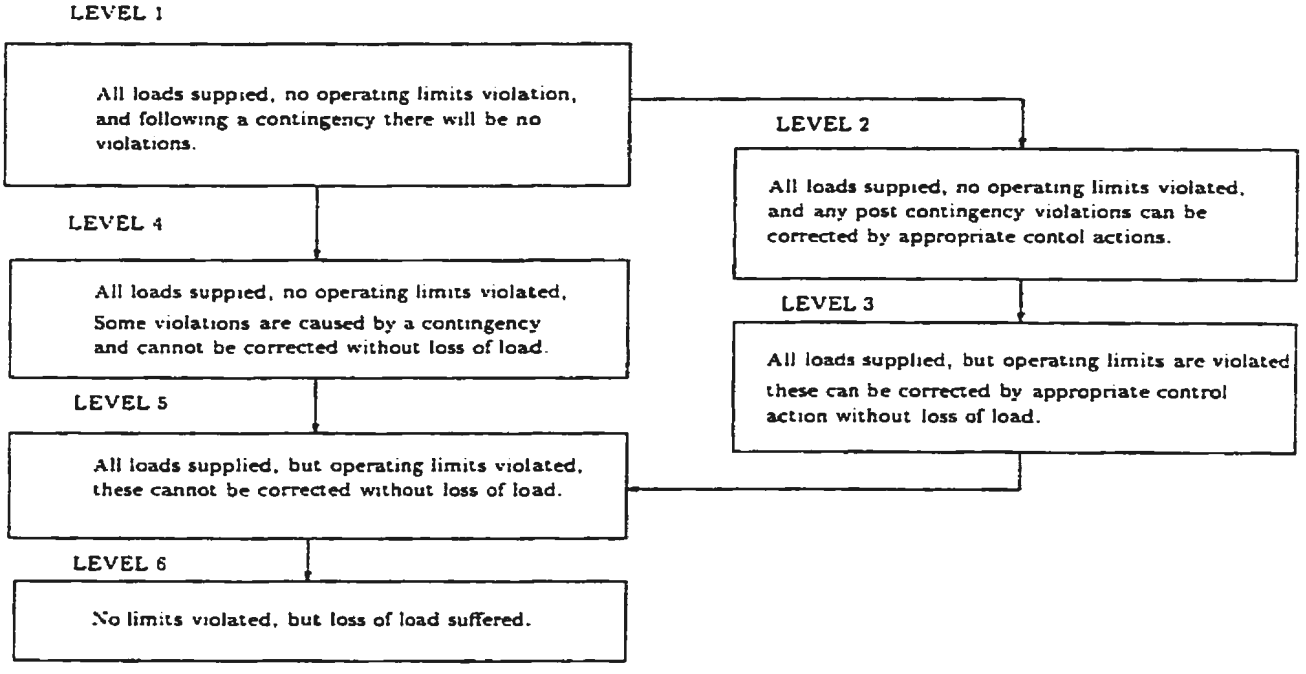

Figure 3.1: Power system static security levels

Levels 1-5 represent the various levels of transition which may occur in the event

of a contingency. Level 6 refers to the severe condition where the system will suffer a loss in loads. SCOPF is normally concerned with level 1 and level 2 security. These levels are defined as follows:

- Security level 1 is one where all the loads are supplied, system is well within its operating limits and no violations occur following a contingency.
- Security level 2 is one where all the loads are supplied, system operates within its limit and the post-contingency violations in the system can be corrected by suitable control actions without loss of load.

Its is more expensive to operate the system at security level 1 compared to security level 2.

3.3 Advantages of SCOPF

The advantages of SCOPF can be demonstrated with the help of a simple example adopted from reference [31]. This two bus system with 2 generators and 2 transmission lines is shown Figure 3.2. The system supplies a total generation of 200 MW at bus 2. The transmission line losses are not considered. The generation limits, line limits and the incremental cost data are:

Generator No.	:	1	2
min. generation (MW)	:	50	0
max. generation (MW)	:	200	120
max. Line limits (MW)	:	120	100
Incremental cost $(\$/MW)$	:	1.0	1.5

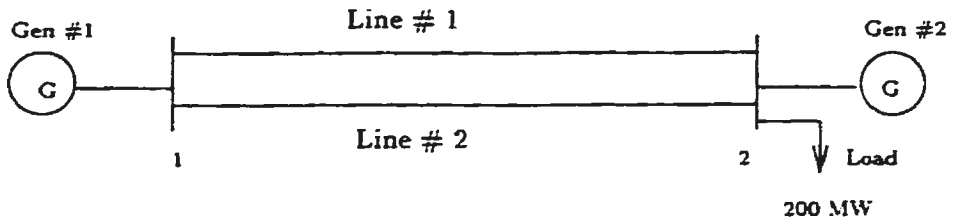

Figure 3.2: Two bus system

If the generation is scheduled using optimal power flow to minimize the operation cost, generator 1 will be assigned the total load of 200 MW. The system operation would be as in Figure 3.3. Under this condition the system is operating in the most economic manner. It can be noted that line 2 is operating at its maximum limit. If the system is subjected to the outage of line 2, the total load power of 200 MW will flow through line 1. As the maximum limit of line 1 is 120 MW, protective relays will disconnect the line and the system will lose its total load.

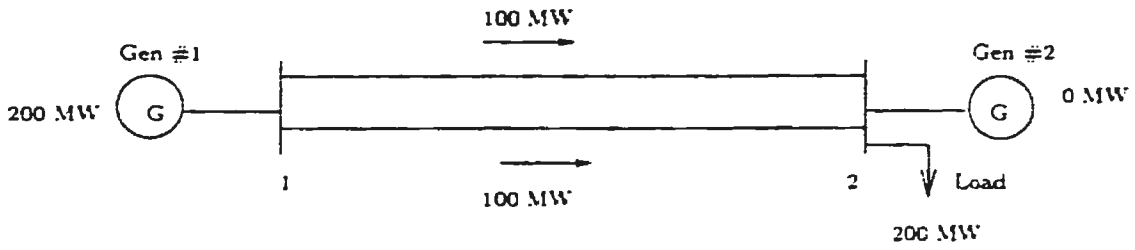

Figure 3.3: OPF solution

Suppose the generators are re-scheduled using SCOPF as shown in Figure 3.4. the system maintains the operation following the outage of line 2 since the remaining line can carry the required power. In this simple example only the line limits are considered. But in a typical system. several system limits are violated following a contingency. The SCOPF takes into account all the system operating limitations.

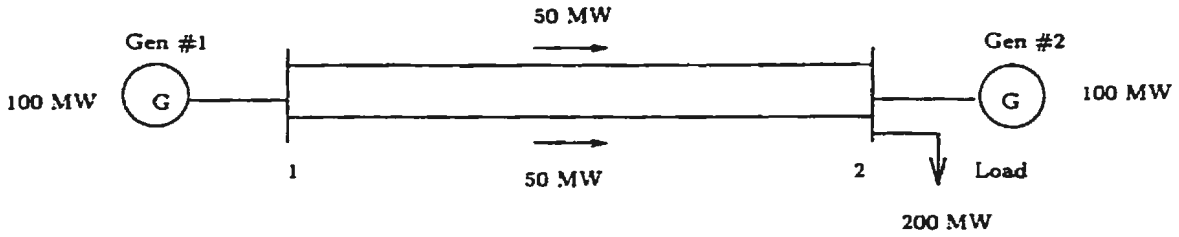

Figure 3.4: SCOPF solution

3.4 Types of Security Constrained Optimal Power Flow

In this section the two basic types of security level 1 SCOPF namely (i) The Non-decomposed approach [4]and (ii) The Decomposed approach [32]are discussed. These methods are based on the formulation of the SCOPF.

3.4.1 The Non-decomposed approach

The SCOPF problem is formulated as a large single multi-variable, multi-constrained optimization problem as in [4]. The main challenge in this method lies in the computational aspect. The SCOPF problem size increases with the number of contingencies considered. If there are N_c contingencies to be considered in the SCOPF, the problem size becomes $N_c + 1$ times as large as the base case OPF. This method requires efficient optimization algorithms to handle the large number of variables and constraints.

3.4.2 The Decomposed approach

In this method the base case optimal power flow is augmented by a small number of post-contingency inequality constraints, expressed in terms of the base case variables as in [32]. The base case OPF problem is first solved separately. Then a contingency

analysis is performed to detect the post-contingency states and the post-contingency violating quantities are linearized about its relevant state and transformed into a function of base-case variables. This is accomplished by using large-perturbation sensitivity analysis, normally by employing Inverse Matrix Modification Lemma [33]. Finally the base-case problem with the augmented post-contingency constraints problem is solved. This cyclic process is repeated till no post-contingency violations occur in the system. This process mainly relies on the fast contingency screening and detection algorithms.

3.4.3 Formulation of Security Constraint Optimal Power Flow

In this section, a non-decomposed SCOPF method is used as in [4]. In this method, the OPF problem is expanded to include the contingency constraints. In general SCOPF formulation can be written as follows:

$$\begin{aligned}
&\textit{Minimize} && f(u^0, x^0) && && (3.1)\\
&\textit{Subject to} && g^0(u^0, x^0) = 0 && && (3.2)\\
& && h^0(u^0, x^0) \leq 0 && && (3.3)\\
& && g^k(u^0, x^k) = 0 && k = 1, 2....N_c && (3.4)\\
& && h^k(u^0, x^k) \leq\ 0 && k = 1, 2....N_c && (3.5)
\end{aligned}$$

where

N_c : *is the total number of contingency cases.*

superscript '0' : *refers to the pre − contingency case.*

superscript 'k' '': *refers to the contingency case.*

In the SCOPF formulation, equations (3.2) - (3.4) represent the base-case OPF problem, which is discussed in detail in chapter 2. This problem is augmented with a set of equality and inequality constraints to reflect each of the contingencies. This method is aimed at obtaining level 1 security. Hence the control variables (u) are taken to be the same as those of the base-case operating condition for all the outage cases.

The set of equality constraints (equation (3.4)) represents the power balance equation for each of the outage cases. The set of inequality constraints (equation (3.5)) represents the system operating limits for each outage cases. The limits of the inequality constraints corresponding to the outage cases need not be the same as the base-case problem. The inequality constraints is discussed in detail in the OPF formulation in chapter 2.

3.5 Computational Aspects

The SCOPF problem was formulated using C++ and solved using MINOS. The major computational problem in solving the SCOPF arises when the number of contingencies to be considered is high. In such a case MINOS requires an initial guess very close to the actual solution for convergence. Hence the problem was solved in two steps. In the first step 1, the SCOPF problem was solved with unbounded Q_g limits. The solution from step 1 was taken as the starting point for step 2. In step 2 SCOPF problem was solved with appropriate limits for Q_g. The tap changing transformers are considered as continuous variables. The slack generator is not considered as a control variable and it is assumed to take the excess generation during the outage cases.

3.6 Simulation Results

The SCOPF results are given for a 6-bus system [29] and the modified IEEE 30-bus system [4].

The voltage limits for all loads are taken as 0.95 to 1.05 p.u. for both the base-case and the contingency cases. The tap settings are allowed to vary between the limits 0.9 to 1.1. Figure 3.5 shows the results of the OPF for the 6 bus system. Although the system is operating at a minimum cost, following the outage of line 2-5 the voltages at bus 3 and bus 5 are violated. The contingency load flow solution is shown in Figure 3.6.

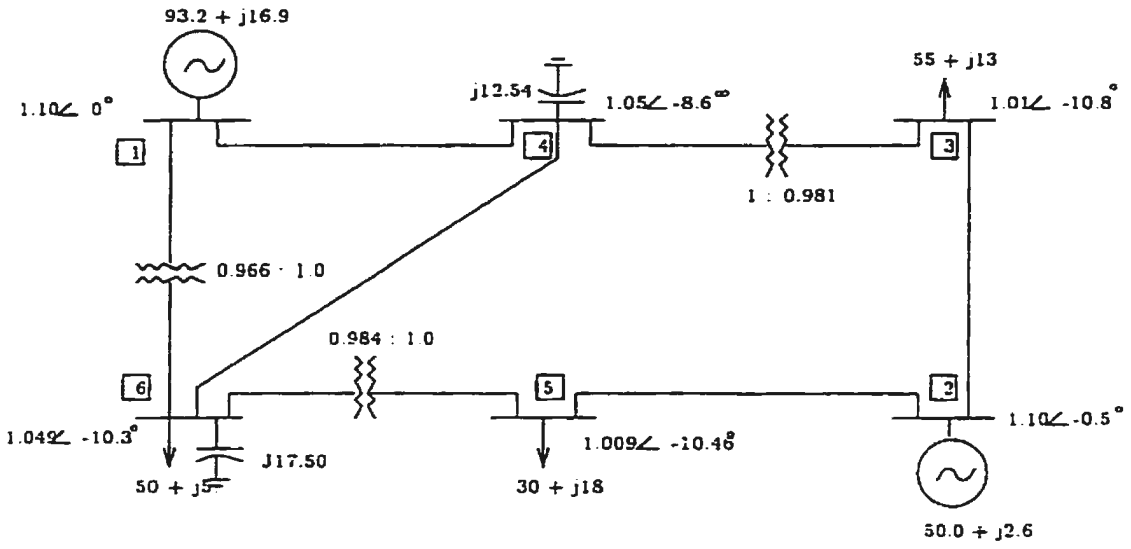

Figure 3.5: OPF solution for 6-bus system

Figure 3.7 shows the SCOPF solution for the 6-bus system including security constraints for the outage of line 2-5. In the SCOPF the control variables are scheduled in such a way that following the outage of the line 2-5 the system will be operating within its limits.The operating cost is higher for SCOPF compared to the

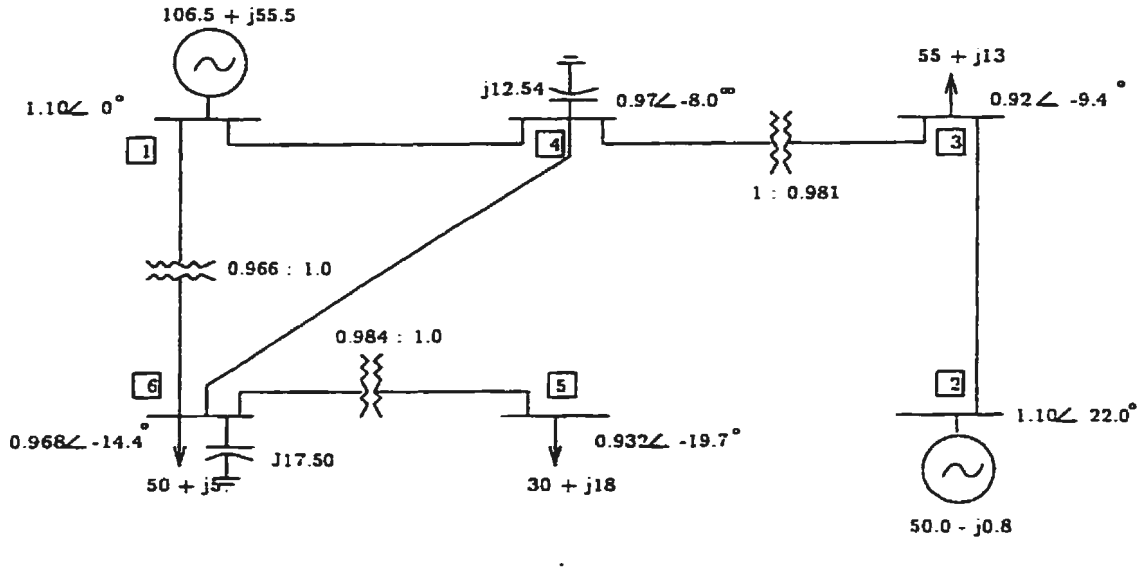

Figure 3.6: Contingency load flow for 6-bus system (for opf)

OPF. However the system will be operating in a more secure manner compared to the OPF.

The contingency load flow solution for the SCOPF solution (outage of line 2-5) is shown in the figure 3.9. All the load bus voltages remain within the operating limits. Table 3.1 summarizes the results for the 6-bus system. In the simulation of the IEEE 30-bus system, 3 pre-selected line outages are considered. The results are shown in Table 3.2. The simulation results show that for the base case and the OPF solution some of the voltages, line flows and reactive power limits are violated following the contingencies. In this example all the load bus voltage limits are considered to be between the range 0.95 and 1.05 for both the base-case and contingencies. The tap settings are allowed to vary in the range of 0.9 to 1.1. Table 3.2 compares the results of SCOPF with OPF and base case load flow solution. It can be noted that in the SCOPF solution the outage of the lines does not violate any of the system operating limits. The SCOPF enhances the security of the system.

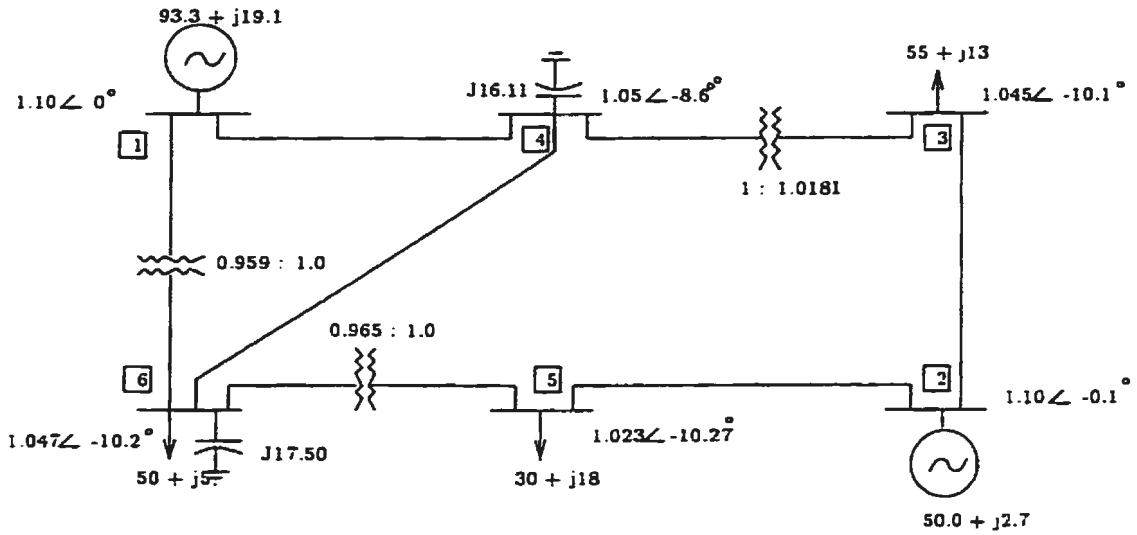

Figure 3.7: SCOPF solution for 6-bus system

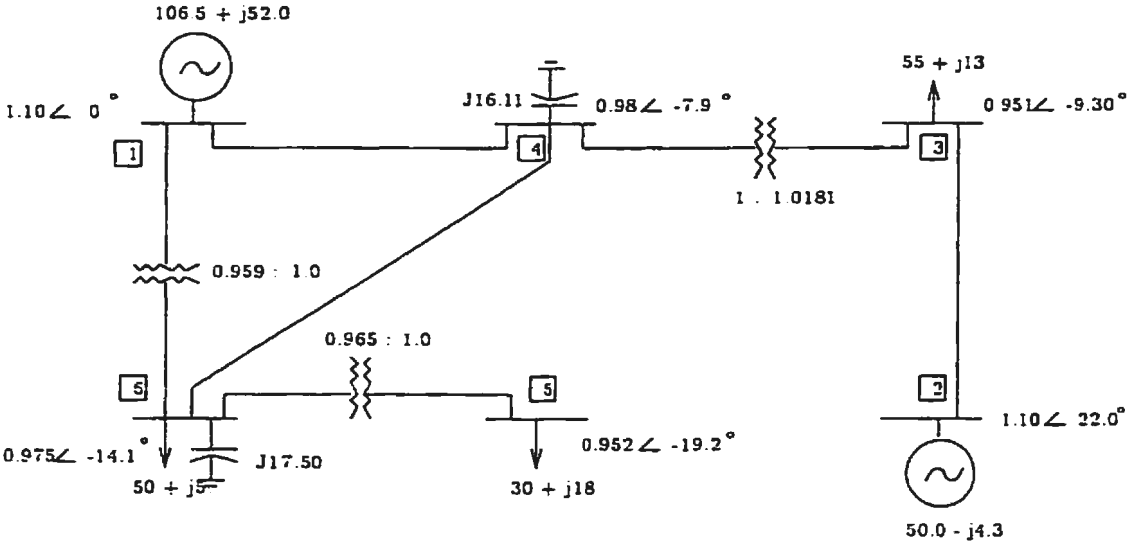

Figure 3.8: Contingency load flow for 6-bus system (for SCOPF)

Table 3.1: SCOPF results for the 6-Bus system

Control variables	BASE CASE	OPF	SCOPF
V_1 (p.u)	1.1	1.1	1.1
V_2 (p.u)	1.1	1.1	1.1
P_{G_2} (MW)	50.0	50.0	50.0
Q_{c_4} (Mvar)	14.4	12.54	16.11
Q_{c_6} (Mvar)	15.6	17.50	17.50
T_1	0.991	0.9657	0.9593
T_2	0.944	0.9847	0.9651
T_3	1.013	0.9810	1.0181
Operating cost ($/hr)	604.58	601.25	602.11
Line outages	Violating quantities		
2-5	V_3 V_5	V_3 V_5	No Violations

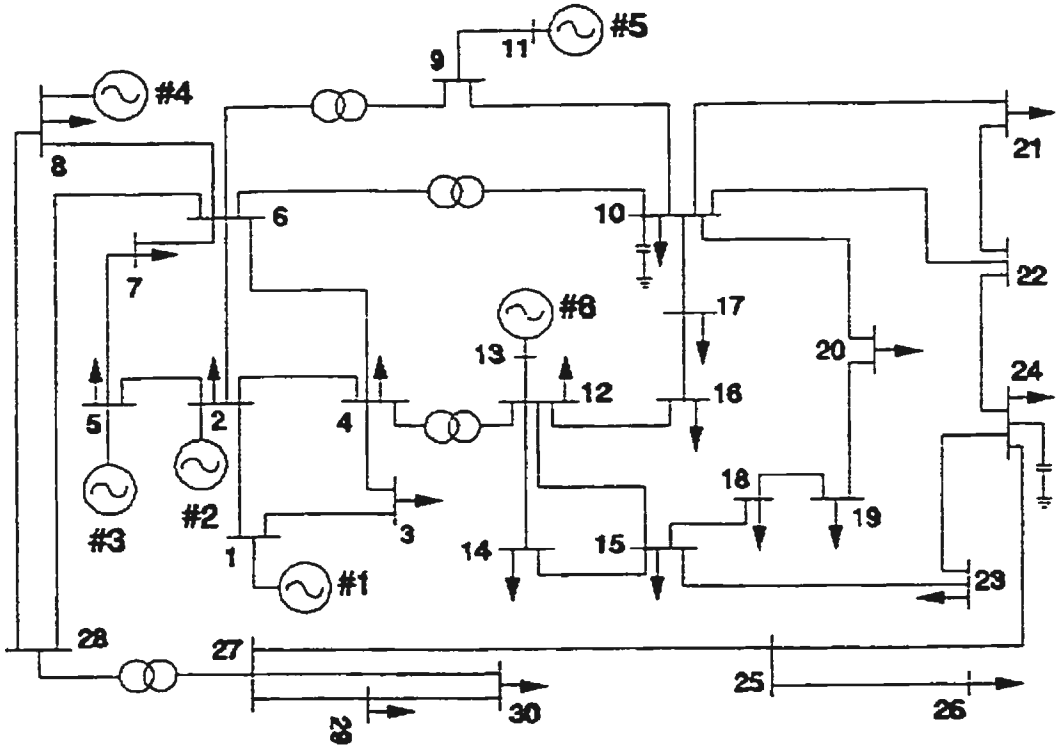

Figure 3.9: Modified IEEE 30-Bus system.

Table 3.2: SCOPF results for the IEEE 30-Bus system

Control variables	BASE CASE	OPF	SCOPF
V_1 (p.u)	1.0500	1.0500	1.0492
V_2 (p.u)	1.0450	1.0381	1.0372
V_5 (p.u)	1.0100	1.0114	0.9872
V_8 (p.u)	1.0100	1.0191	1.0213
V_{11} (p.u)	1.0500	1.0891	1.1000
V_{13} (p.u)	1.0500	1.0858	1.0827
P_{G_2} (MW)	80.0	48.56	60.11
P_{G_5} (MW)	50.0	21.43	27.68
P_{G_8} (MW)	20.0	21.70	35.00
$P_{G_{11}}$ (MW)	20.0	12.06	20.41
$P_{G_{13}}$ (MW)	20.0	12.00	19.41
T_1	0.9780	1.0018	1.0418
T_2	0.9690	1.0468	1.0824
T_3	0.9320	1.0011	0.9950
T_4	0.9680	0.9425	0.9422
Operating cost ($/hr)	903.3	800.79	822.06
Line outages	Violating quantities		
1-3	Q_1	Q_1, I_1	No Violations
4-6	V_{12}	Q_1, I_1	
2-5	V_9	I_5, I_7	

3.7 Summary

This chapter has presented the formulation of SCOPF to maintain the economy and security of the power system following a contingency. The formulation of security constraints in OPF makes it a more powerful tool for system operation and planning. Simulation results were provided for a 6 bus system and 30 bus system. Operating cost of the SCOPF are slightly higher compared to the OPF. However in SCOPF, following the outage of the lines the system will be within its operating limits. The

increase in the operating cost is greatly offset by the enhancement in the security of the system. In some cases the line outages may even lead to a total blackout and result in the loss of millions of dollars. It should be noted that there is always a trade-off between security and economy.

Chapter 4

Voltage Stability

4.1 Introduction

Recently, voltage stability has become an important issue to electric power utilities as the utilities are operating very close to its limits due to economical and environmental constraints [10]. This chapter presents the theory of voltage stability and the analytical tools used to study the voltage stability problem. This chapter also discusses three different voltage stability indices in detail and simulation results based on these indices are presented for sample power systems namely, the 6-bus system and a 30-bus system.

4.2 Definitions

Voltage stability involves a wide range of phenomenon and it is considered as a separate subject of study [35]. Voltage stability is different from the rotor angle stability (transient stability). Voltage stability is viewed as a *load stability*, and rotor angle stability is basically *generator stability*. Some of the terms which are often related with voltage stability are [11]:

- *Voltage Stability* is the ability of a system to maintain voltage so that when load admittance is increased, load power will increase, and both the power and

voltage are controllable.

- *Voltage Collapse* is the process by which voltage instability leads to a very low voltage profile in a significant part of the system.

- *Voltage Security* is the ability of a system, not only to operate stably, but also to remain stable following any reasonably credible contingency or adverse system change.

4.3 Mechanism of Voltage Collapse

The mechanism of voltage collapse can be explained by considering a radial system [11] shown in Figure 4.1. This system is mainly consists of two loads, (i) industrial load and (ii) residential load. These loads have different characteristics. A major portion of the industrial load is made up of induction motors which operate at low power factor. These loads are not significantly affected by voltage variations. Residential loads on the other hand operate at higher power factor and are affected by change in voltage.

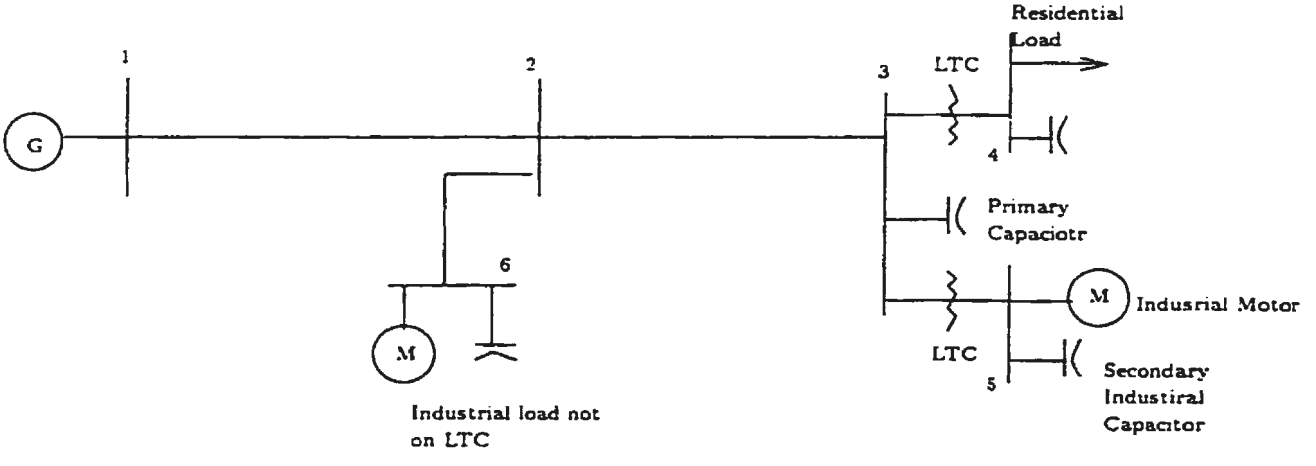

Figure 4.1: Radial system used to demonstrate the voltage collapse mechanism

Voltage collapse may be triggered by a small increase in load or loss of transmission line or generation. This will cause the receiving end voltage to drop. The total residential load will reduce as the voltage drops. The industrial load will not be affected much by this drop in voltage. The reactive power compensation devices in the industrial load will decrease its reactive power contribution. Hence there will be a net increase in the reactive power demand in the industrial load. But this is greatly offset by the net decrease in the residential load. As a result the voltage will settle at a low value, nearly 95% of its initial value.

When the voltage near the load decreases the transformer LTC's will come into action and it will try to increase the voltage near the receiving end. This causes the residential load to increase and draw more reactive power. The increasing residential load will cause the primary voltage of the transformer to fall further. The reactive power compensating devices connected to the primary will produce less reactive power and the primary reactive losses will increase. This will cause the voltage to drop and settle at a value near 90 % of the nominal voltage.

A major portion of the residential load is made up of heating load. The thermostats in the heater will try to increase the load to maintain the output power. This will cause the voltage to further drop. As the voltage falls below a nominal accepted value the induction motors in the industrial load will stall. This will increase the reactive current drawn by these motors and this may lead to a total voltage collapse. This total scenario may take a few minutes to hours. In the event of a severe contingency the voltage collapse may be faster.

4.4 Static vs Dynamic Analysis

There has always been a debate on whether voltage stability is a static or dynamic phenomenon. The time frame for the static and dynamic stability are not the same. The time frame for the dynamic voltage stability is in the order of milliseconds to few seconds, while the static voltage stability occurs in the time frame of several minutes to hours. The three major components which play an important role in the voltage stability are the tap-changer dynamics, load dynamics and the generator excitation dynamics. Hence, voltage stability is a dynamic process. Various aspects of the static and dynamic voltage stability have been discussed in [36] and it has been pointed out that both the static and dynamic approaches lead to the same results under certain conditions. Voltage stability has often been viewed as a steady state aspect considering the longer time frame involved. Most of the tools used to analyze the voltage stability problem in the utilities are based on the static model of the power system. Hence in our discussion we have focused our interest on the static voltage stability methods.

4.5 Methods of Voltage Stability Analysis

The two widely used methods for voltage stability analysis are: (i) P-V curves and (ii) V-Q curves. These two methods are based on the conventional power flow analysis.

4.5.1 P-V curves

P-V curves are obtained by plotting the total system load (P) versus the voltage of the critical bus (V). These curves are plotted from the results obtained from the load flow solutions by slowly increasing the loads in discrete steps. Figure 4.2 shows

the P-V curves. P-V curves are parabolic in shape. In the top half of the curve, the voltage decreases as the system load increases. Here the slope of the curve is negative. The nose point (normally referred to as the critical point) of the curve gives the maximum power which can be delivered to the load. The bus voltage corresponding to the critical point is referred to as the *critical voltage*. Out of all the buses in the system, the voltage profile of one particular bus will approach the critical point faster compared to the other buses. The voltage stability of the system is limited by this particular bus. The voltage profile of this particular bus is used to study the stability of the system and it is referred as the *critical bus* for the system. A disadvantage in this P-V curves is that near the critical point the power flow Jacobian matrix tends to be singular and the power flow solutions starts to diverge near this point. Hence special tools such as the Continuation Power Flow [37] should be used to obtain the load flow solution near the critical point.

The P-V curves are also used to determine the voltage stability margin of the system. *Voltage stability margin* can be considered as the amount of additional load in a specific pattern of load increase that would cause a voltage collapse in the system. This can be estimated from the P-V curves as the difference (in MW) between the critical point and the base case loading.

Figure 4.2 shows the P-V curves for different power factors. As the power factor changes the critical point varies. The critical point is higher for a leading power factor compared to a lagging power factor. Also the critical voltage is higher for a leading power factor. This is an important aspect in voltage stability.

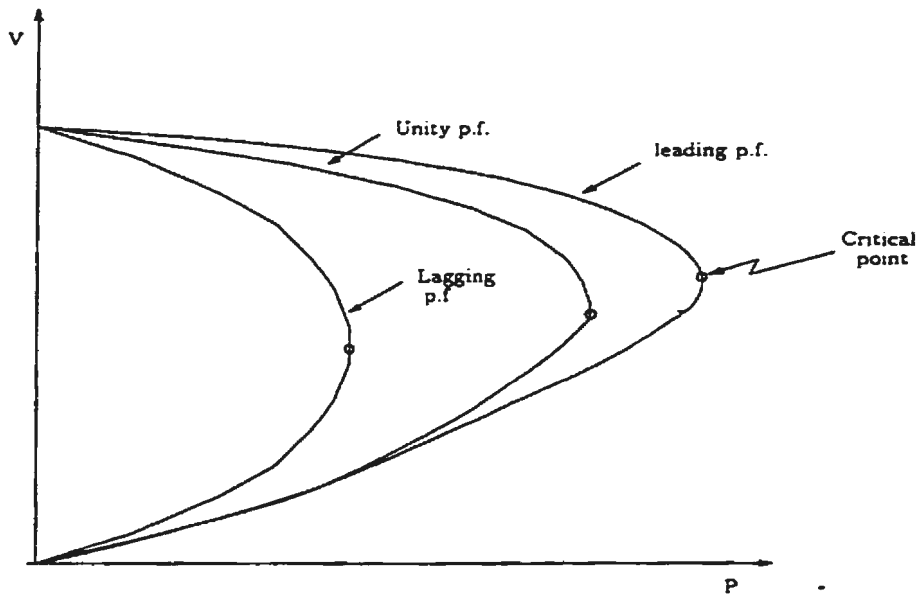

Figure 4.2: P-V curves

4.5.2 V-Q curves

The V-Q curves are plots of the critical bus voltage versus reactive power of the same bus. To obtain the V-Q curve of a bus, a fictitious synchronous condenser is represented at that particular bus and the bus is assumed to be a voltage controlled bus without reactive power limits. A series of power flow simulations are done for various values of synchronous condenser voltage and the corresponding reactive power output is obtained. The V-Q curves are obtained by plotting the condenser reactive power output versus the voltage. The voltage is taken as the independent variable. From this curve the operating point can be obtained by removing the fictitious synchronous condenser, which corresponds to the zero reactive power point in the plot. Some of the main advantage of the V-Q curves are:

- As the voltage stability problem is closely related to the reactive power, the reactive power margin can be directly obtained from this curves. This is the

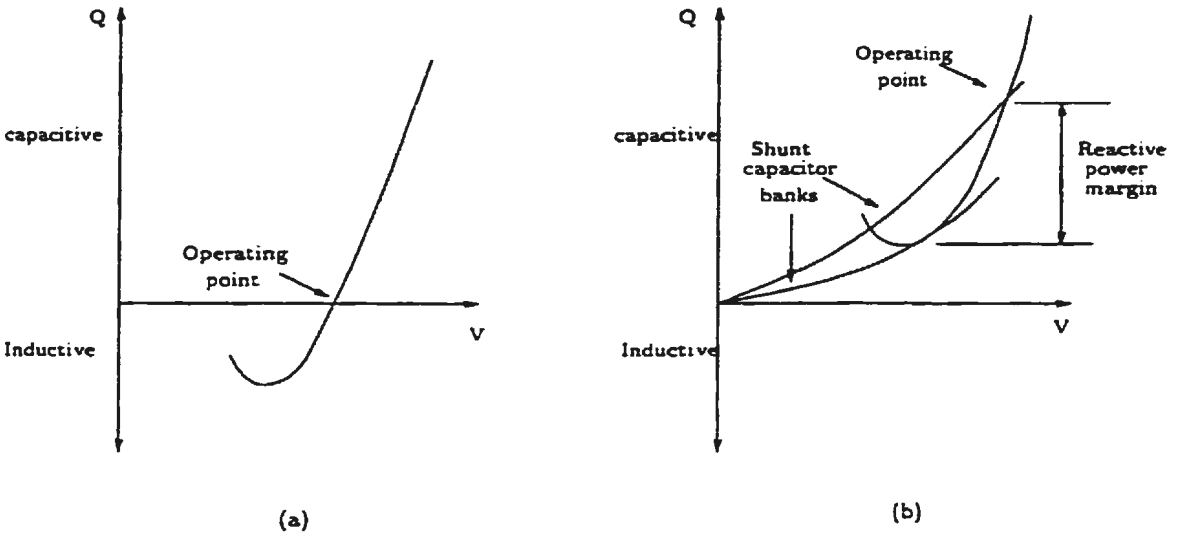

Figure 4.3: V-Q curves

margin between the operating point and the bottom point of the curve as shown in Figure 4.3(a).

- The characteristics of the shunt compensating devices can be directly plotted on the same plots. In this case the reactive power margin is calculated as the distance between the operating point and the point at which the compensating device characteristics is tangent to the V-Q curves. This is shown in the Figure 4.3(b).

V-Q curves are widely used in utilities to analyze the voltage stability problem.

There are a number of tools used to evaluate the steady state voltage stability limit of the system. Three of such tools which are widely used are discussed here, namely:

1. Continuation Power Flow.

2. Minimum Singular Value method.

3. Kessel and Glavitch method.

4.6 Continuation Power Flow

The key idea in Continuation Power Flow (CPF) [37] is to avoid the singularity of the Jacobian of the power flow problem by slightly reformulating the power flow equation to include a load parameter, and apply the locally parameterized continuation technique.

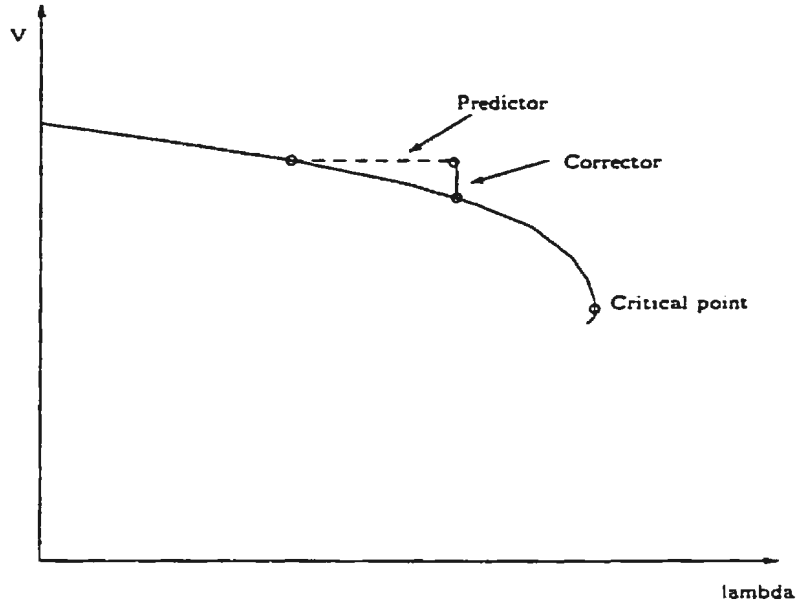

Figure 4.4: Continuation Power Flow

As shown in Figure 4.4, CPF starts with a known solution and uses a tangent predictor to estimate the next solution. This estimate is then corrected using a Newton-Rapson technique.

The power flow equations in general can be written as

$$F(\underline{x}, \lambda) = 0 \tag{4.1}$$

where $x = [\underline{\delta}, \underline{V}]^T$ and λ represents the load parameter such that

$$0 \leq \lambda \leq \lambda_{critical} \tag{4.2}$$

where $\lambda = 0$ corresponds to the base case and $\lambda = \lambda_{critical}$ corresponds to the critical point.

The dimension of F will be $2n_{pq} + n_{pv}$, where n_{pq} and n_{pv} are the number of PQ and PV buses respectively, which may be written as follows

$$P_{Gi}(\lambda) - P_{Li}(\lambda) = \sum_{j \epsilon i} V_i V_j (G_{ij} cos\theta_{ij} + B_{ij} sin\theta_{ij}) \quad i = 1, 2 ..... n_{pq} + n_{pv} \tag{4.3}$$

$$Q_{Gi}(\lambda) - Q_{Li}(\lambda) = \sum_{j \epsilon i} V_i V_j (G_{ij} sin\theta_{ij} + B_{ij} cos\theta_{ij}) \quad i = 1, 2 ..... n_{pq} \tag{4.4}$$

where

$$P_{Gi}(\lambda) = P_{Gio}(1 + \lambda K_{Gi}) \tag{4.5}$$

$$P_{Li}(\lambda) = P_{Lio}(1 + \lambda K_{Li}) \tag{4.6}$$

$$Q_{Li}(\lambda) = Q_{Lio}(1 + \lambda K_{Li}) \tag{4.7}$$

P_{Lio} , Q_{Lio} : *active and reactive loads at bus i in the base case.*

P_{Gio} : *active power generation at bus i in the base case.*

K_{Li} : *constant used to specify the rate of load increase at bus i as λ varies.*

K_{Gi} : *constant used to specify the rate of generation increase as λ varies.*

The base case solution of the above equation is the ordinary power flow solution with $\lambda = 0$. Once this is calculated it should be continued for the case ((x_1, λ_1), (x_2, λ_2), ...$(x_{critical}, \lambda_{critical})$). CPF uses a predictor-corrector scheme to find the continuum of power flow solution.

4.6.1 Prediction

The prediction of the next solution can be made by taking an appropriate sized step in the direction tangent to the solution path. The tangent calculation is derived by taking the derivative of both sides of equation (4.1)

$$dF = \frac{\partial F}{\partial \delta} d\delta + \frac{\partial F}{\partial V} dV + \frac{\partial F}{\partial \lambda} d\lambda = 0 \tag{4.8}$$

The tangent vector is obtained as

$$\begin{bmatrix} \underline{F_\delta} & \underline{F_V} & \underline{F_\lambda} \end{bmatrix} \begin{bmatrix} d\delta \\ dV \\ d\lambda \end{bmatrix} = 0 \tag{4.9}$$

In equation (4.9) the matrix [F] is the Jacobian matrix augmented with an additional column (f_λ), and $t = [d\delta, dV, d\lambda]^T$ is the tangent vector . The addition of λ has increased the number of unknowns, while the number of equations remain unchanged. The problem is solved by adding one more equation which consists of a non-zero magnitude for one of the tangent vectors to equation (4.10). The resulting equation is

$$\begin{bmatrix} \underline{F_\delta} & \underline{F_V} & \underline{F_\lambda} \\ & \underline{e_k} & \end{bmatrix} \begin{bmatrix} d\delta \\ dV \\ d\lambda \end{bmatrix} = 0 \tag{4.10}$$

The tangent vector is calculated by solving equation (4.10) and the predictor is made as shown in equation (4.11)

$$\begin{bmatrix} \delta^* \\ V^* \\ \lambda^* \end{bmatrix} = \begin{bmatrix} \delta \\ V \\ \lambda \end{bmatrix} + \sigma \begin{bmatrix} d\delta \\ dV \\ d\lambda \end{bmatrix} = 0 \tag{4.11}$$

where σ designates the step size.

4.6.2 Parameterization and Corrector

In the parameterization, the original power flow equations are augmented by one more equation that specifies the value of one of the state variables. The new set of equations is given in equation (4.12) and it is solved by Newton-Rapson method.

$$\begin{bmatrix} \underline{F}(x) \\ x_k - \eta \end{bmatrix} = 0 \tag{4.12}$$

There are several ways of choosing the continuation parameter. Usually the state variable with the greatest rate of change near a given point is chosen as the continuation parameter. The best way to evaluate the continuation parameter is as shown in equation (4.13).

$$x_k : \|t_k\| = max \|t_1\|, \|t_2\|, ...\|t_m\| \tag{4.13}$$

While selecting the continuation parameter the sign should be noted so as to assign +1 or -1 for the subsequent tangent vector calculation.

The CPF is used as an bench mark to obtain the PV-curves. VSTAB [38] was used to obtain the PV-curves. VSTAB is a commercial software used to analyze the voltage stability and contingency load flow.

Simulation results are obtained for the 6-bus system and the IEEE 30-bus system. Figures 4.5 and 4.6 show the PV-curve for the critical bus for these systems.

Table 4.1: CPF for the 6-bus system

Total Load (MW)	Voltage at Bus 3	Voltage at Bus 4	Voltage at Bus 5	Voltage at Bus 6
135.00	1.0106	1.0496	1.0099	1.0489
165.00	0.9554	1.0029	0.9401	0.9978
195.00	0.8829	0.9407	0.8478	0.9286
225.00	0.7672	0.8387	0.6986	0.8125
232.50	0.7120	0.7885	0.6257	0.7534
234.37	0.6922	0.7702	0.5988	0.7312
236.25	0.6560	0.7360	0.5480	0.6885
236.37	0.6525	0.7326	0.5427	0.6841
236.41	0.6443	0.7236	0.5291	0.6708
236.63	0.6362	0.7158	0.5159	0.6600
236.70	0.6286	0.7083	0.5030	0.6492
236.80	0.6215	0.7008	0.4904	0.6383
236.46	0.6152	0.6946	0.4782	0.6285
236.21	0.6098	0.6890	0.4662	0.6193
235.79	0.6048	0.6835	0.4545	0.6098
235.21	0.6004	0.6785	0.4432	0.6005
232.49	0.5967	0.6740	0.4321	0.5913

As discussed in the previous sections, critical bus for the system is the one where the voltage declines much faster than the other load buses. The voltage declines for all the load buses in the 6-bus system is shown in Table 4.1. From this table it can be seen that Bus 5 is more critical compared to the other buses. Similarly for the 30 bus system, Bus 30 was the most critical bus out of all the 24 load buses.

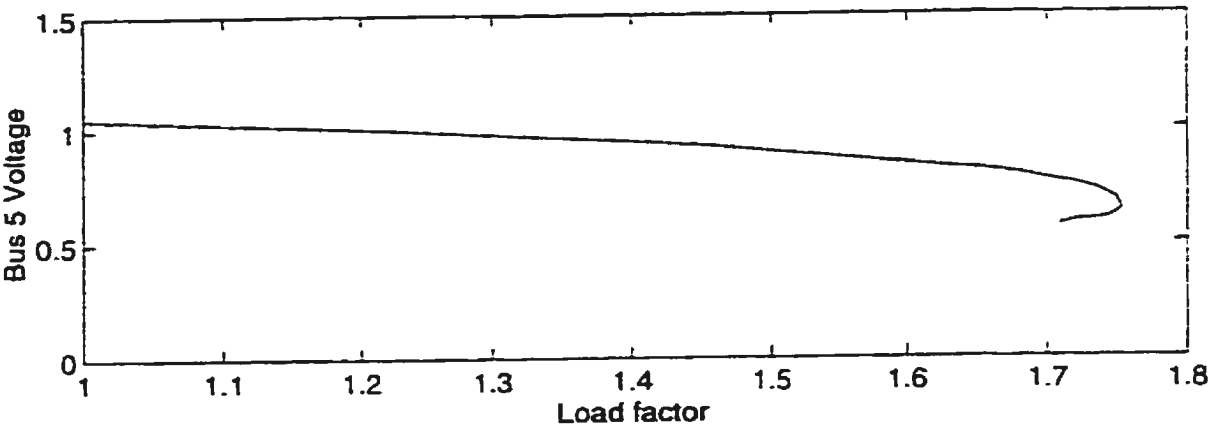

Figure 4.5: Continuation Power Flow for the 6-bus system

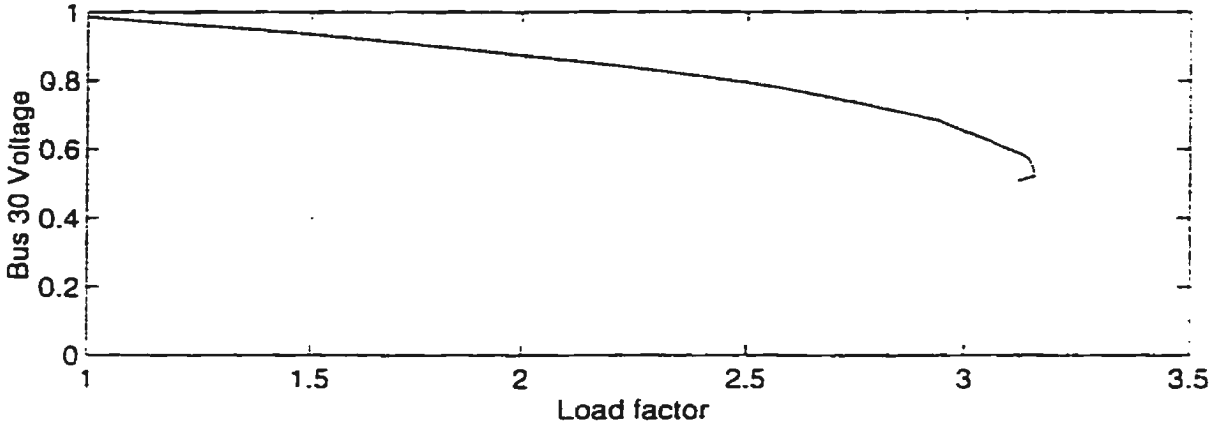

Figure 4.6: Continuation Power Flow for the 30-bus system

4.7 Minimum Singular Value method

The use of singularity of the power flow Jacobian as an indicator for steady state voltage stability was first proposed by Venikov et al.[39], where the sign of the determinant of the Jacobián was used to determine whether the system is stable or

not. At the static bifurcation point the Jacobian becomes singular and the inverse of the Jacobian does not exists. In 1988, Tiranuchit et al.[15] proposed a static voltage stability index based on the minimum singular value of the power flow Jacobian.

The power flow equations are written as in equations (4.14) and (4.15):

$$\underline{P}(\delta, V) = 0 \tag{4.14}$$

$$\underline{Q}(\delta, V) = 0 \tag{4.15}$$

where P and Q represent the set of active and reactive power balance equation of the system. The power flow Jacobian matrix is given by

$$\underline{J}(V, \delta) = \begin{bmatrix} \frac{\partial P}{\partial \delta} & \frac{\partial P}{\partial V} \\ \\ \frac{\partial Q}{\partial \delta} & \frac{\partial Q}{\partial V} \end{bmatrix} \tag{4.16}$$

The singular value decomposition of the Jacobian matrix is obtained by

$$\underline{J} = \underline{U}\ \underline{\Sigma}\ \underline{V^T} \tag{4.17}$$

where U and V are the orthogonal matrices. $\Sigma = diag[\sigma_1, \sigma_2 ..... \sigma_n]$ with $\sigma_{max} = \sigma_1 \geq \sigma_2 ..... \geq \sigma_n = \sigma_{min}$

The minimum singular value is the security index to monitor how close the system is to voltage stability.

This method was implemented using MATLAB. Results for the Minimum Singular Value index for the 6-bus system and the IEEE 30-bus system are shown in the Figures 4.7 and 4.8 respectively. It can be noted that the minimum singular value of the Jacobian matrix starts to decrease from the base case load and reach a value of zero near the critical point.

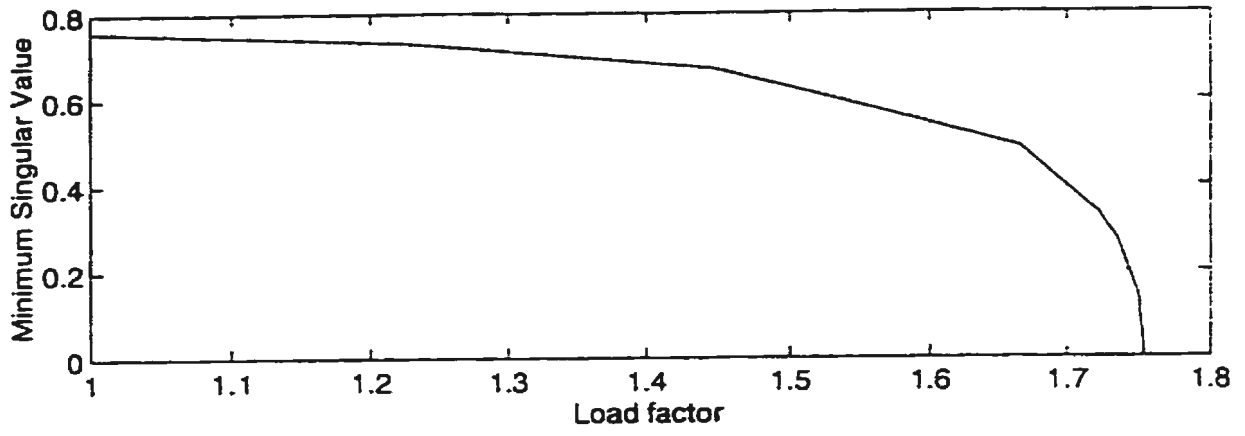

Figure 4.7: Minimum Singular Value for the 6-bus system

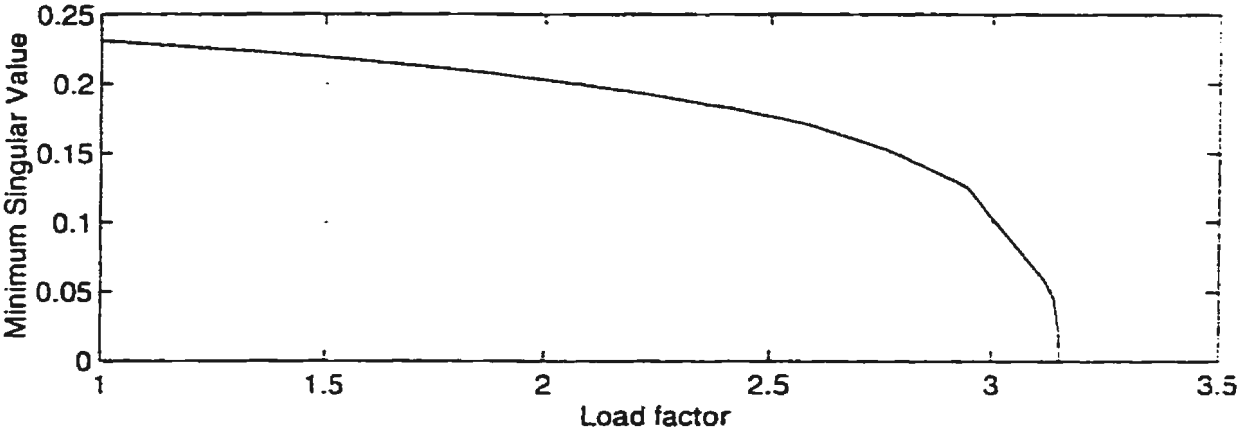

Figure 4.8: Minimum Singular Value for the 30-bus system

4.8 Kessel and Glavitch method

Kessel and Glavitch [40] developed a voltage stability index based on the feasibility of power flow equations for each node. The multi-node power system is represented as two categories of nodes, one which is characterized by the behavior of PQ-node and the other by the PV-node. This is represented in terms of a hybrid matrix as given in equations (4.18) and (4.19):

$$\begin{bmatrix} V_L \\ I_G \end{bmatrix} = \begin{bmatrix} H \end{bmatrix} \begin{bmatrix} I_L \\ V_G \end{bmatrix} \tag{4.18}$$

$$\begin{bmatrix} V_L \\ I_G \end{bmatrix} = \begin{bmatrix} Z_{LL} & F_{LG} \\ K_{GL} & Y_{GG} \end{bmatrix} \begin{bmatrix} I_L \\ V_G \end{bmatrix} \tag{4.19}$$

where

V_L , I_L vector of voltages and currents of the customer nodes.

V_G , I_G vector of voltages and currents of the generator nodes.

The H-matrix is generated by the partial inversion of the YBUS. For the PQ node, the voltage V_j is given by

$$V_j = \sum_{i \epsilon a_l} Z_{ji} I_i + \sum_{i \epsilon a_g} F_{ji} V_i \tag{4.20}$$

The global indicator L is given by [40]

$$L = max \| 1 - \frac{\sum_{i \epsilon a_g} F_{ji} V_i}{V_j} \| \tag{4.21}$$

The L-indicator varies in the range between 0 (for no-load) to 1 (voltage collapse point). This index was implemented using MATLAB. Results for a 6 bus system and the IEEE 30 bus system are shown in the Figures 4.9 and 4.10 respectively.

The figure compares the L-index performance is compared with the CPF results. It can be seen that the L-index reaches the value of 1 near the voltage collapse point. Although the L-index value slightly exceeds the theoretical value of 1 near the point of collapse. the effect of this error with respect to the load factor is very small.

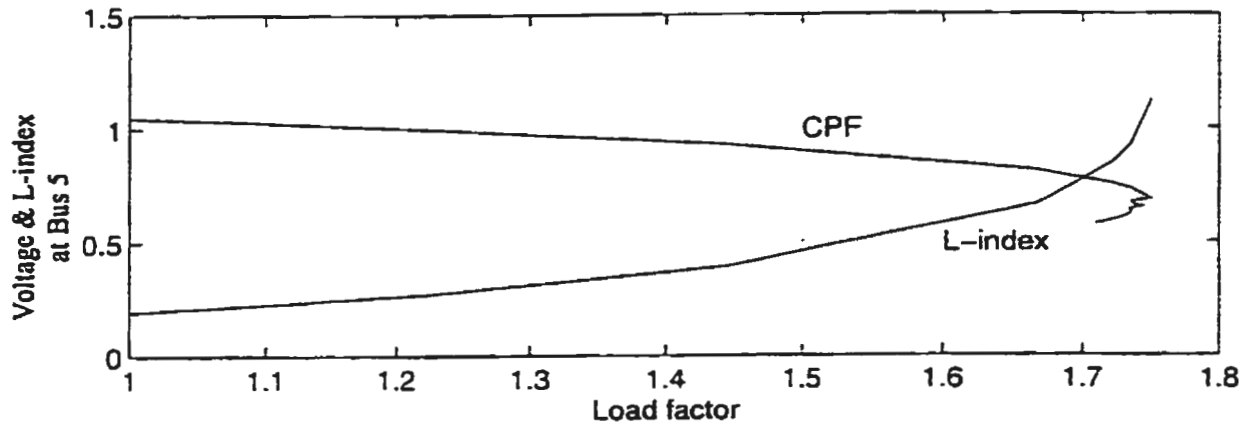

Figure 4.9: L-index for the 6-bus system

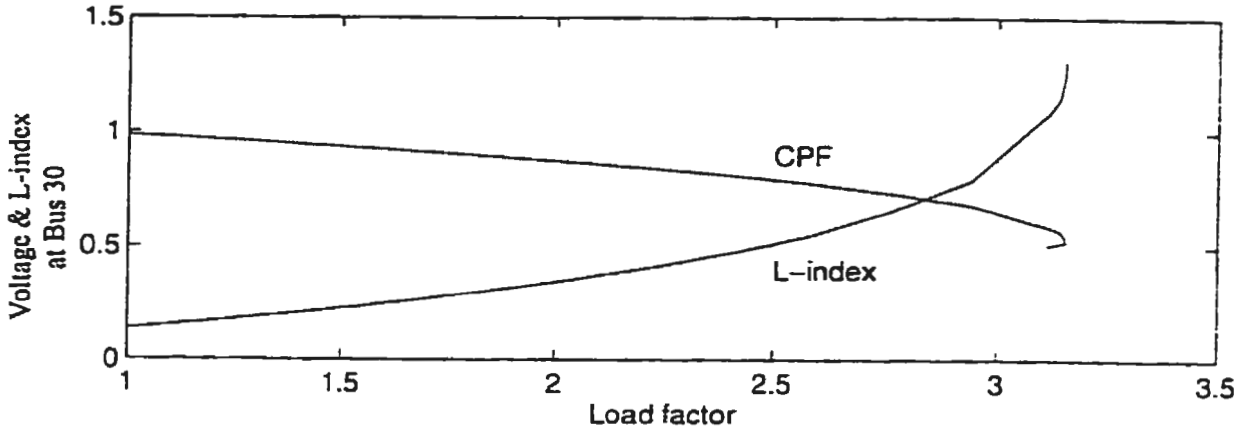

Figure 4.10: L-index for the 30-bus system

4.9 Summary

This chapter has presented a discussion on the theory and analytical tools used to study the voltage stability problem. Three different types of voltage stability indices namely Continuation Power Flow (CPF), Minimum Singular Value and L-index are discussed. Simulation results are presented for a 6 bus system and 30 bus system for the three methods. CPF is used as a benchmark in the power utilities to determine the stability margin and evaluate the other indices. The Voltage stability index

based on the Minimum Singular Value is used by some utilities to study the voltage stability problem. The main disadvantage of this method is the computation time. The L-index based voltage stability index is simple to compute and it provides a means to judge the voltage stability of the system at any given operating point. Simulation results based on the L-index are compared with the CPF results for the 6 bus system and 30 bus system. It can be noted that the L-index does not need the computation of Jacobian matrix. In chapter 5, the L-index based voltage stability index has been used to investigate the effects of the voltage stability index in SCOPF.

Chapter 5

Optimal Power Flow including Voltage Stability

5.1 Introduction

In recent years increased loading and exploitation of transmission lines for economic reasons have created voltage stability problems in all major utilities. Chapters 2, 3 and 4 have discussed the significance of optimal power flow, security constrained optimal power flow and voltage stability in the power system operation. Security constrained OPF is a class of OPF problem which takes into account the security of the system following a contingency. However, in the present SCOPF problem the voltage stability of the system has not been taken into account. This chapter proposes a method to include the voltage stability index as a part of OPF. The advantages of the proposed method are discussed with the simulation results for the test power systems.

5.2 Optimal Power Flow including Voltage Stability Index

To include the voltage stability index as a part of the OPF, the index must be simple to calculate and it should give a clear picture of how close the system is operating

with respect to the voltage collapse point. Most of the indices are based on the load flow solution and use sensitivity of Jacobian matrix to evaluate the voltage stability of the system. This kind of sensitivity based indices involves the computation of the inverse of the Jacaobian matrix and it is not easy to include such indices as a part of OPF. The L-index proposed by Kessel and Glavitsch [40] and discussed in chapter 4 is simple to calculate and it does not require the calculation of the Jacobian matrix. The value of the index varies from 0 to 1 between no load to critical load. This gives a clear idea how close the system is from the point of collapse.

The L-index can be formulated as a part of the OPF as

$$Minimize \quad f(u,x) \tag{5.1}$$

$$Subject\ to \quad g(u,x) = 0 \tag{5.2}$$

$$h(u,x) \leq 0 \tag{5.3}$$

$$l(u,x) \leq 1 \tag{5.4}$$

Equations (5.1) to (5.3) represent the general OPF formulation as discussed in chapter 2, equation (5.4) refers to the L-index for each of the load bus in the system. The L-index is calculated as shown in equation (5.5)

$$L = max\|1 - \frac{\sum_{i\epsilon\alpha_g} F_{ji}V_i}{V_j}\| \tag{5.5}$$

where

$$V_j = \sum_{i\epsilon\alpha_l} Z_{ji}I_i + \sum_{i\epsilon\alpha_g} F_{ji}V_i \tag{5.6}$$

The values of Z_{ji} and F_{ji} are obtained from the partial inversion of the YBUS. The various computations involved in calculating the L-index are discussed in detail in chapter 4, where it is shown that the L-index can be computed independently. The main advantage of formulating the L-index as part of OPF is discussed in the following sections.

5.3 Voltage Stability Margin Enhancement

The main objective of including the voltage security index in OPF is to improve the voltage stability margin. The voltage security index in the OPF allows one to improve the voltage stability margin of the system to be improved in two ways. The L-index can be formulated as a part of the OPF constraints.This will allow the operator to restrict the value of the L-index within a range of 0 to L_{max}. In the other method, the value of the L-index can be minimized by formulating the index as the objective function of the OPF. This will minimize the value of the L-index of the most critical bus in the system and will result in a better voltage stability margin. These two methods are discussed in the following sections:

5.3.1 L-index as OPF constraints

Voltage collapse often occurs in a stressed system operating at a higher loading condition. In such a operating condition some of the system parameters will be operating close to their limits and following a contingency these parameters will violate the system limits. Hence it is not possible to maintain the level 1 security of the system as discussed in SCOPF in chapter 3. In the discussion here, the security of the post-contingency system is viewed in terms of voltage stability of the system. The main aim is to avoid the possibility of voltage instability of the system following

a contingency. Figure 5.1 show the CPF plot for the 6-bus system. The plots shows the voltage at bus 5 corresponding to the base case and the outage of line 2-5. Figure 5.2 shows the CPF results for the 30-bus system. the plot shows the voltage profile of bus 30 system corresponding to the base case and outage of line 38.

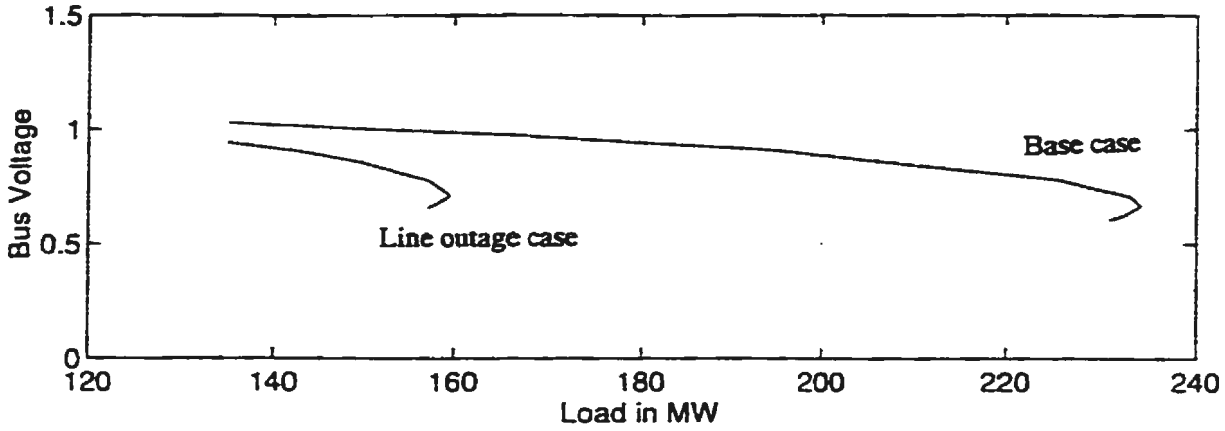

Figure 5.1: Continuation Power Flow for the base case and a line outage case for the 6 bus system

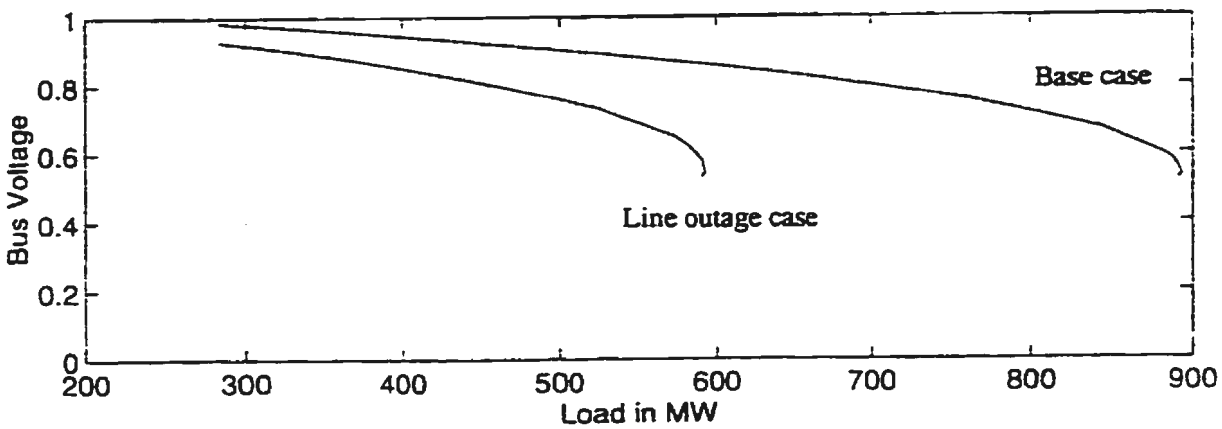

Figure 5.2: Continuation Power Flow for the base case and a line outage case for the 30 bus system

It can be seen that the voltage stability margins of the system are determined by the outage case, as its voltage profile reaches the critical point much earlier compared to the base case. At a particular loading condition the stability margin may be adequate for the base case solution. However if a contingency occurs in the

system the voltage stability margin of the system may be marginal for the post-contingency operating condition. In some cases this may lead to voltage instability.

In this OPF formulation, the security of a stressed power system is viewed as follows:

- the pre-contingency operating condition should be within the specified system limits.
- the post-contingency operating condition should be maintained away from the critical point.

The OPF formulation with L-index as constraints is given as follows:

$$\begin{aligned}
Minimize \quad & f(u^0, x^0) && (5.7)\\
Subject\ to \quad & g^0(u^0, x^0) = 0 && (5.8)\\
& h^0(u^0, x^0) \leq 0 && (5.9)\\
& l^0(u^0, x^0) \leq 1 && (5.10)\\
& g^k(u^0, x^k) = 0 \qquad k = 1, 2.....N_c && (5.11)\\
& h^k(u^0, x^k) \leq 0 \qquad k = 1, 2.....N_c && (5.12)\\
& l^k(u^0, x^k) \leq L_{max} \qquad k = 1, 2.....N_c && (5.13)
\end{aligned}$$

where

N_c : *is the total number of contingency cases.*

superscript 0 : *refers to the pre – contingency case.*

superscript k : *refers to the contingency case.*

This formulation is similar to the non-decomposed SCOPF as discussed in chapter 3 with slight modifications. It includes an additional set of inequality constraints (5.10) and (5.13), which represent the L-index for each of the load buses in the system. The base case formulation represented by the superscript '0' is same as the general OPF formulation with all the system limits as discussed in chapter 2. For the contingency case represented by superscript 'k', the set of inequality constraints are different from the base case. For the contingency case only the following inequality constraints are considered:

- Limits of the real and reactive power generation at the Generator buses.

$$P_{G_{low_i}} \leq P_{G_i} \leq P_{G_{high_i}} \tag{5.14}$$

$$Q_{G_{low_i}} \leq Q_{G_i} \leq Q_{G_{high_i}} \tag{5.15}$$

- Limits on the tap setting of the transformers.

$$t_{low_i} \leq t_i \leq t_{high_i} \tag{5.16}$$

- Limits on the shunt capacitance and reactances.

$$s_{low_i} \leq s_i \leq s_{high_i} \tag{5.17}$$

As the voltage stability margin of the system is determined by the contingencies in the system, the limits of the L-index following a contingency is not allowed to exceed the value of L_{max}. The value of L_{max} is fixed at a value less than 1 and depends on the operating condition.

5.3.2 L-index as OPF objective

In this method the value of the L-index for the most critical bus in the system is taken as the objective function. When the system is operating close to the critical

point, the objective function of OPF is replaced with the L-index of the most critical bus in the system and the optimal power flow problem is solved. The new OPF formulation is given as:

$$Minimize \quad |1 - \frac{\sum_{i \in \alpha_g} F_{ji} V_i}{V_j}|^* \tag{5.18}$$

$$Subject\ to \quad g^0(u^0, x^0) = 0 \tag{5.19}$$

$$h^0(u^0, x^0) \leq 0 \tag{5.20}$$

$$l^0(u^0, x^0) \leq 1 \tag{5.21}$$

$$g^k(u^0, x^k) = 0 \qquad k = 1, 2....N_c \tag{5.22}$$

$$h^k(u^0, x^k) \leq 0 \qquad k = 1, 2....N_c \tag{5.23}$$

$$l^k(u^0, x^k) \leq L_{max} \qquad k = 1, 2....N_c \tag{5.24}$$

where

N_c : *is the total number of contingency cases.*

superscript '0' : *refers to the pre − contingency case.*

superscript 'k' : *refers to the contingency case.*

The '*' in the objective function refers to the value of the L-index for the most critical bus out of all the contingency case. This is the L-index with the maximum value out of all the L-index constraints. The L-index is basically expressed as a function of the state and control variables.

5.4 Simulation Results

Most of the test systems used to demonstrate the OPF and SCOPF represent the base case loading conditions. To evaluate the proposed L-index based OPF methods,

a stressed system at higher loading condition is required. Due to the lack of such standard test systems, the loads and generations of the standard 6 bus system and the IEEE 30 bus systems are increased as in Continuation Power Flow [37] analysis. A load parameter λ is defined as

$$0 \leq \lambda \leq \lambda_{critical} \tag{5.25}$$

where $\lambda = 0$ corresponds to the base case and $\lambda = \lambda_{critical}$ corresponds to the critical point.

For a given value of λ the change in the loading conditions for the system is given by

$$P_{Li} = P_{Lio}(1 + \lambda K_{Li}) \tag{5.26}$$

$$Q_{Li} = Q_{Lio}(1 + \lambda K_{Li}) \tag{5.27}$$

where

P_{Lio} , Q_{Lio} : *active and reactive loads at bus i in the base case.*

K_{Li} : *constant used to specify the rate of load increase at bus i as* λ *varies.*

The real and reactive power generation limits in the system are modified as

$$P_{Gi_{max}} = P_{Gio_{max}}(1 + \lambda K_{Gi}) \tag{5.28}$$

$$P_{Gi_{min}} = P_{Gio_{min}}(1 + \lambda K_{Gi}) \tag{5.29}$$

$$Q_{Gi_{max}} = Q_{Gio_{max}}(1 + \lambda K_{Gi}) \tag{5.30}$$

$$Q_{Gi_{min}} = Q_{Gio_{min}}(1 + \lambda K_{Gi}) \tag{5.31}$$

where

P_{Gio} , Q_{Gio} : *active and reactive loads at bus i in the base case.*

K_{Gi} : *constant used to specify the rate of generation increase as* λ *varies.*

5.4.1 6-Bus system

The 6-bus system has 2 generators, 3 tap-changing transformers, 2 capacitor banks and 7 lines. The line data, bus data and generator data for the system are given in Appendix B. The total base case load of the system is 135 MW. The total load of the system is increased by 27 MW. The real and reactive power load on all the load buses are increased as mentioned in equations (5.26) and (5.27).

Table 5.1: OPF with L-index for the 6-Bus system

Control variables	Values
V_1 (p.u)	1.1
V_2 (p.u)	1.1
P_{G_2} (MW)	56.80
Q_{c_4} (Mvar)	16.50
Q_{c_6} (Mvar)	17.50
T_1	0.9183
T_2	0.9827
T_3	0.9535
Operating cost [$/hr]	887.31
L-index value (at Bus 5)	0.8115
Stability [MW] Margin	15.47

All the real and reactive generation limits are increased as given by equations (5.28) to (5.31). The voltage magnitude limits for the base case for all the generator buses are between 0.95 and 1.1 p.u. For all the load buses the voltage magnitudes limits are between 0.95 to 1.05 p.u. The simulation results discussed in chapter 4 indicate that bus 5 is the most critical bus for this system. For this system the voltage stability margin is limited by the outage of line 5. Hence in this formulation only the outage of line 5 is considered.

Table 5.2: OPF with L-index (L_{max}=0.75) for the 6-Bus system

Control variables	Values
V_1 (p.u)	1.1
V_2 (p.u)	1.1
P_{G_2} (MW)	56.80
Q_{c_4} (Mvar)	16.50
Q_{c-6} (Mvar)	17.50
T_1	0.9009
T_2	0.9495
T_3	0.9574
Operating cost [$/hr]	$89.13
L-index value (at Bus 5)	0.7500
Stability [MW] Margin	18.75

The results of the OPF with L-index is summarized in Table 5.1. The objective of this OPF is to minimize the total operating cost of the system. The L-index value is 0.8115 at bus 5 for the outage of line 5. This indicates that the system is operating close to the voltage collapse point. To confirm this the voltage stability margin from

this operating point was calculated using the CPF method for the outage of line 5. The voltage stability margin of the system at this operating condition was calculated to be 15.47 MW.

The results of OPF with L-index with constraint limit ($L_{max} = 0.75$) is summarized in Table 5.2. The results indicate that the L-index value of the bus 5 reaches the maximum limit of 0.7500. The voltage stability margin was found to be 18.75 MW. It can be seen that as the L-index value is forced by the constraints upper limit of 0.75 at bus 5 compared to the value of 0.8115 in the previous case, the voltage stability margin is improved.

Table 5.3: OPF with L-index as objective function for the 6-Bus system

Control variables	Values
V_1 (p.u)	1.1
V_2 (p.u)	1.1
P_{G_2} (MW)	54.51
Q_{c_4} (Mvar)	16.50
Q_{c-6} (Mvar)	17.50
T_1	0.9000
T_2	0.9152
T_3	0.9643
Operating cost [$/hr]	913.41
L-index value (at Bus 5)	0.7146
Stability [MW] Margin	20.62 MW

The results of OPF with L-index of bus 5 as objective function is summarized in Table 5.3. In this method the value of the L-index at the bus 5 for the outage case

is minimized. The L-index was reduced to a value of 0.7145. The voltage stability margin was found to be 20.62 MW. It can be noted that the total operating cost of the system has increased. But the increase in the cost can be justified by the increase in the voltage stability margin of the system.

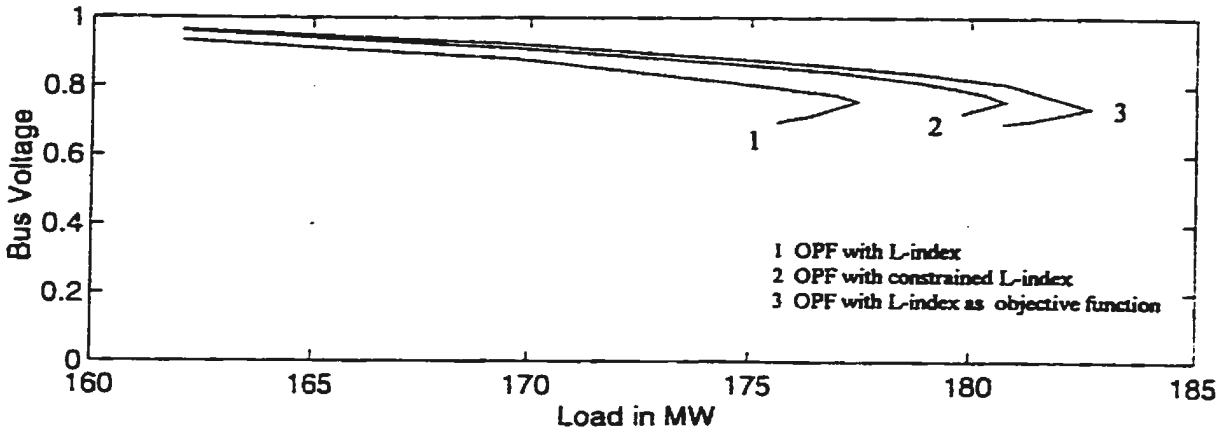

Figure 5.3: P-V curves (CPF method) for the 6 bus system

Figure 5.3 shows the P-V curves (CPF method) which is used to determine the voltage stability margin for the three different approaches discussed and summarized in Table 5.4.

Table 5.4: Comparison of OPF results with voltage stability index for 6-Bus system

Method	Value of L-index	Stability Margin (MW)
OPF with L-index	0.8115	15.47
OPF with L-index (L_{max}=0.75)	0.7500	18.75
OPF with L-index as Objective fn.	0.7146	20.26

5.4.2 30-Bus system

The 30-Bus system has 6 generators, 4 tap-changing transformers, 2 capacitors and 41 lines. The line data, bus data and generation data for the system are given in Appendix B. The total base case load of the system is 283.4 MW. The total system load is increased by 250 MW. The load increase is distributed among all the load buses as in equations (5.26) and (5.27).

Table 5.5: OPF with L-index for the 30-Bus system

Control variables	Values
V_1 (p.u)	1.1000
V_2 (p.u)	1.0772
V_5 (p.u)	1.0274
V_8 (p.u)	1.0413
V_{11} (p.u)	1.1000
V_{13} (p.u)	1.1000
P_{G_2} (MW)	81.97
P_{G_5} (MW)	33.48
P_{G_8} (MW)	54.30
$P_{G_{11}}$ (MW)	38.50
$P_{G_{13}}$ (MW)	35.92
T_1	0.9959
T_2	1.1000
T_3	0.9927
T_4	0.9087
Operating cost [$/hr]	1823.27
L-index value (at Bus 30)	0.8150
Stability [MW] Margin	2.20 MW

The real and reactive power generation in the system is increased as mentioned in equations (5.28) to (5.31). The voltage magnitude limits for the voltage controlled buses are between 0.95 to 1.10 p.u. The voltage magnitude limits for all the remaining buses are between 0.95 and 1.05 p.u.

Table 5.6: OPF with L-index (L_{max}=0.8000) for the 30-Bus system

Control variables	Values
V_1 (p.u)	1.1000
V_2 (p.u)	1.0786
V_5 (p.u)	1.0358
V_8 (p.u)	1.0450
V_{11} (p.u)	1.1000
V_{13} (p.u)	1.0902
P_{G_2} (MW)	88.25
P_{G_5} (MW)	33.69
P_{G_8} (MW)	54.30
$P_{G_{11}}$ (MW)	37.98
$P_{G_{13}}$ (MW)	36.02
T_1	1.0044
T_2	1.1000
T_3	0.9764
T_4	0.9108
Operating cost [$/hr]	1823.50
L-index value (at Bus 30)	0.8000
Stability [MW] Margin	2.5 MW

Simulations results of CPF for the system as discussed in chapter 4 indicate that the bus 30 is the most critical bus in this system. The voltage stability margin of this system is limited by the outage of line 38. Only the outage of line 38 is considered

in the OPF formulation.

The results of the OPF with L-index is summarized in Table 5.5. The objective of this OPF is to minimize the total operating cost of the system. The total operating cost of the system was 1823.27 $/hr. The L-index value was 0.8120 and the voltage stability margin from this operating point was calculated to be 2.2 MW.

Table 5.7: OPF with L-index as objective function for the 30-Bus system

Control variables	Values
V_1 (p.u)	1.0792
V_2 (p.u)	1.0664
V_5 (p.u)	1.0774
V_8 (p.u)	1.0571
V_{11} (p.u)	1.1000
V_{13} (p.u)	1.1000
P_{G_2} (MW)	122.22
P_{G_5} (MW)	23.46
P_{G_8} (MW)	28.61
$P_{G_{11}}$ (MW)	46.60
$P_{G_{13}}$ (MW)	61.90
T_1	1.1000
T_2	0.9000
T_3	0.9572
T_4	0.9029
Operating cost [$/hr]	1939.23
L-index value (at Bus 30)	0.7694
Stability [MW] Margin	19.0 MW

The results of the OPF with L-index with constraint limits of L_{max}=0.8000 is summarized in Table 5.6. The L-index of the critical bus 30 reaches the maximum

limit of 0.8000. The voltage stability margin of the system was found to be 2.50 MW. The total cost of operation of the system was $ 1823.50 / hr.

The results of OPF with L-index as objective function for the 30 bus system is summarized in Table 5.7. Here the L-index of bus 30 corresponding to the outage of line 38 is minimized. The L-index value was minimized to a value of 0.7694. The voltage stability margin was found to be 19.0 MW. It can be noted that the total operating cost of the system has increased, however the new voltage stability margin is much higher compared to the previous margins.

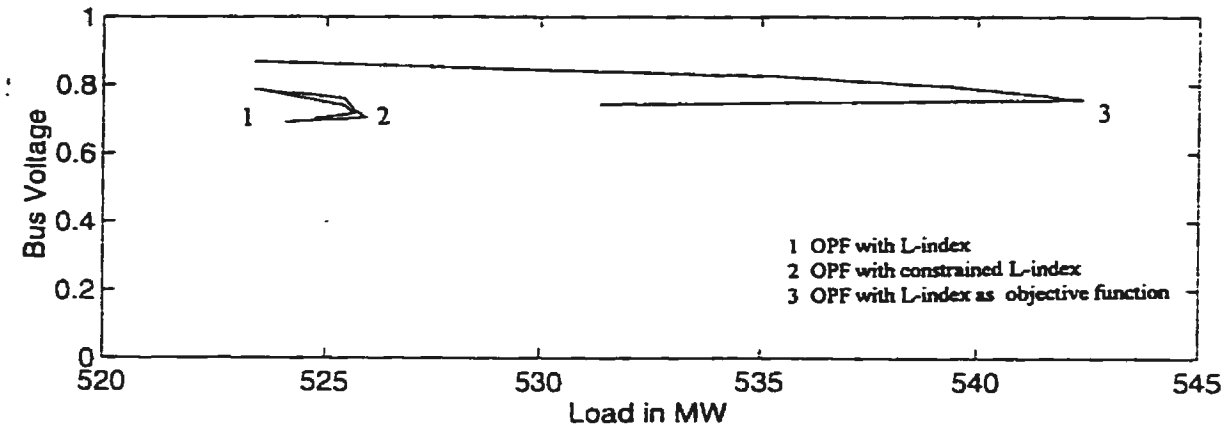

Figure 5.4: P-V curves (CPF method) for the 30 bus system

Figure 5.4 shows the P-V curves (CPF method) for the 30 bus system, which is used to determine the voltage stability margin for the three different approaches discussed. The results are summarized in Table 5.8.

Table 5.8: Comparison of OPF results with voltage stability index for 30-Bus system

Method	Value of L-index	Stability Margin (MW)
OPF with L-index	0.8150	2.20
OPF with L-index (L_{max}=0.80)	0.8000	2.50
OPF with L-index as Objective fn.	0.7694	19.0

5.5 Summary

This chapter has presented a method to include the voltage stability index as a part of OPF. An L-index based voltage stability index has been formulated as a set of constraints. The formulation of L-index as a part of OPF constraints allows the operator to set the limits on the L-index of the most critical bus in the system and this helps the system to be operated away from the voltage collapse point. The simulation results are discussed for a 6 bus system and 30 bus system. It can be noted that by restricting the value of L-index constraints, the stability margin of the system is improved.

The L-index was also formulated as the objective function and minimized to improve the stability margin. In this formulation the L-index of the most critical bus was taken as the objective function. The simulation results are presented for a 6 bus system and 30 bus system. The results show that minimizing the L-index of the critical bus results in an improved stability margin.

Chapter 6

Conclusions

6.1 Contributions of the Research

This thesis has studied the Optimal Power Flow (OPF) problem in detail and an OPF program has been developed to solve the power flow problem, which is capable of handling two different objective functions: one to minimize the total operating cost and another to minimize the total system losses. The OPF simulation results are presented on test power systems. In the second phase of the research the advantages of Security Constrained Optimal Power Flow (SCOPF) over the OPF have been investigated. A SCOPF program has been developed and simulation results for SCOPF are presented for a 6 bus system and the modified IEEE 30 bus system.

The major contributions of the thesis relate to the investigation on the effects of including a voltage stability index as a part of SCOPF. A number of voltage stability indices have been developed in the past few years. This thesis has studied three different types of indices in detail namely, Continuation Power Flow (CPF), Minimum Singular Value and the L-index based voltage stability index. The simulation results based on these three methods are discussed on test power systems. Out of the three indices investigated the L-index based voltage stability index was found to be simple in terms of computation and easy to formulate as a part of OPF.

In the first phase of the investigation, the effects of L-index based voltage stability index as a part of SCOPF constraints has been investigated. The L-index was included as a set of constraints for the base case and for each of the contingencies studied in the SCOPF formulation. The value of the L-index at the end of each SCOPF simulation gives an idea how close the system is operating with respect to the voltage collapse. The effects of restricting the maximum value of the L-index of these constraints was investigated. Simulation results are discussed for a 6 bus system and a 30 bus system. The simulation results shows that restricting the movement of the L-index constraint leads to significant improvement in the voltage stability margin of the system.

In the second phase of the investigation, the effects of including the L-index as a part of SCOPF objective function was studied. The L-index of the most critical bus was used as the objective function and minimized. The simulation results are presented for a 6 bus system and 30 bus system. It was found that minimizing the L-index of the most critical bus has a significant effect on the voltage stability margin of the system.

Both the methods used to investigate the effect of voltage stability index as a part of SCOPF have improved the voltage stability margin of the system. The results of the research shows that by including the voltage stability index as a part of SCOPF, the system can be operated with improved voltage stability margins. This enhances the overall security of the power system with respect to voltage collapse.

6.2 Future Work

The work reported on this thesis can be extended in the following areas:

- Due to the limitations in the computer hardware and software, the present work has been used to demonstrate results for sample test power systems only. This work can be extended to test the results for Electric power utilities.

- Multiple objective optimization algorithms can be used to formulate the voltage security index as an objective function which will result in a better stability margin.

References

[1] H. W. Dommel and W. F. Tinney, "Optimal power flow solutions", *IEEE Trans. on PAS*, vol. 87, October 1969, pp.1866-1876.

[2] M. Huneault and F. D. Galiana, "A survey of the optimal power flow literature", *IEEE Trans. on Power Systems*, vol. 6, no. 2, May 1991, pp.726-770.

[3] B. Stott, O. Alsac and A. J. Monticelli, "Security analysis and optimization", *Proc. of IEEE*, vol. 75, no.12, December 1987, pp. 1623-1644.

[4] O. Alsac and B. Stott, "Optimal load flow with steady-state security", *IEEE Trans. on PAS*, vol. 93, May/June 1974, pp. 745-751.

[5] A. J. Elacqua and S. L. Corey, "Security constrained dispatch at the New York power pool", *IEEE Trans. on PAS*, vol. 101, August 1982, pp. 2876-2884.

[6] J. C. Kaltenbach and L. P. Hajdu, "Optimal corrective rescheduling for power security", *IEEE Trans. on PAS*, vol. 90, no.2, April 1971, pp. 843-851.

[7] L. G. Dias and M. E. El-Hawary, "A preventive strategy method for voltage and reactive power dispatch", *IEEE Trans. on PAS*, vol. 104, no.7, July 1985, pp. 1670-1676.

[8] L. G. Dias and M. E. El-Hawary, "Effect of Load modeling in security constrained OPF studies", *IEEE Trans. on Power Systems*, vol. 6, no. 1, February 1991, pp. 87-93.

[9] L. G. Dias and M. E. El-Hawary, "Security constrained OPF: influence of fixed tap transformer fed loads", *IEEE Trans. on Power Systems*, vol. 6, no. 4, November 1991, pp. 1366-1371.

[10] G. Brownell and H. Clark, "Analysis and solutions for bulk system voltage instability",*IEEE Computer Applications in Power Systems*, July 1989, pp.31-35.

[11] IEEE Committee Report, "Voltage Stability of Power Systems: Concepts, Analytic tools, and Industrial Experience", *IEEE Publications 90TH0358-2-PWR*, 1990.

[12] CIGRE WG 38.02 Task Force No.10, "Modelling of voltage collapse including dynamic phenomena", *Technical report of task force 31-02-10*, CIGRE, June 1992.

[13] H. G. Kwatny, A. K. Pasrija and L. Y. Bahar, "Static bifurcations in electric power networks: loss of steady-state stability and voltage collapse", *IEEE Trans. Circuits and Systems*, vol. 33, no. 10, October 1986, pp. 981-991.

[14] I. Dobson and H. D. Chaing, "Towards a theory of voltage collapse in electric power systems", *Systems & Control Letters*, vol. 13, October 1989, pp. 253-262.

[15] A. Tiranuchit, R. J. Thomas, R. A. Duryea and F. T. Luk, "A posturing strategy against voltage instability in electric power systems ", *IEEE Trans. on Power Systems*, vol. 3, no. 1, February 1988, pp. 87-93.

[16] P. A. Lof, T. Smed, G. Anderson and D. J.Hill, "Fast calculation of a voltage stability index", *IEEE Trans. Power Systems*, vol.7, no. 1, February 1992, pp. 54-64.

[17] H. D. Chiang and R. Jean-Jumeau "Toward a practical performance index for predicting voltage collapse in electric power system", *IEEE Trans. on Power Systems*, vol. 10, no. 2, May 1995, pp. 584-592..

[18] F. Gubina and B. Strmcnik, " Voltage collapse proximity index determination using voltage phasor approach",*IEEE Trans. on Power Systems*, vol. 10, no. 2, May 1995, pp. 788-792.

[19] T. J. Overbye and C. L. DeMarco, " Voltage stability enhancement using energy based sensitivity",*IEEE Trans. on Power Systems*, vol. 6, no. 3, August 1992, pp.1196-1202.

[20] V. Ajjarapu, P. L. Lau and S. Battula, "An optimal reactive power planning strategy against voltage collapse", *IEEE Trans. on Power Systems*, vol. 9, no. 2, May 1993, pp. 906-917.

[21] O. O. Obadina and G. J. Berg, "VAR planning for power system security", *IEEE Trans. on Power Systems*, vol. 4, no. 2, May 1989, pp. 677-686.

[22] M. Begovic, X. Y. Chao and P. S. Meliopoulos, "Voltage stability margin enhancement via optimal power flow", *Proceedings, Bulk Power System Voltage Phenomena II*, Maryland, August 1991, pp.321-331.

[23] H. W. Kuhn, A. W. Tucker, *Non-linear programming, Proc. 2nd Berkeley Symposium on Mathematics, Statistics and Probability*, University of California Press, Berkeley, California, 1951.

[24] D. I. Sun, B. Ashley, B. Brewer, A. Hughes and W. F. Tinney, "Optimal power flow by Newton approach", *IEEE Trans. on PAS*, vol. 103, no. 10, October 1984, pp. 2864-2875.

[25] B. A. Murtagh and M. A. Saunders, "Minos 5.4 User's Guide", *Technical Report SOL 83-20R*, Department of Operations Research, Stanford University, CA 94305-4022, December 1983.

[26] P. Wolfe, "Methods of nonlinear programming", in: J. Abadie, ed. *Nonlinear programming* (North-Holland, amsterdam, 1967), pp. 97-131.

[27] Robert Lafore, *Object-Oriented Programming in Turbo C++*, Galgotia Publications pvt. Ltd., New Delhi 1994.

[28] B. A. Murtagh and M. A. Saunders, "A Projected Lagrangian algorithm and its implementation for sparse nonlinear constraints", *Mathematical Programming Study 16* (1982), pp. 84-117.

[29] B. M. Weedy, *Electric Power System*, 2nd Edition, Wiley and Sons, New York 1971.

[30] P. Kundur, "Power System Stability and Control", McGraw Hill, 1993.

[31] A. Monticelli, M.V.F Pereira and S. Granville, "Security-constrained optimal power flow with post-contingency corrective re-scheduling", *IEEE Trans. on Power Systems*, vol. PWRS-2, February 1987, pp. 175-182.

[32] J. Carpentier, "Differential injection method: A general method for security and optimal load flows", *in IEEE PICA Conf. Proc.(Minneapolis, MN, June 1973)*, pp.255-262.

[33] O. Alsac, B. Stott and W. F. Tinney, "Sparsity-oriented computation methods for modified network solutions.", *IEEE Trans. on PAS*, vol. 102, May 1983, pp. 1050-1060.

[34] D. T. Sun and R. R. Shoults, "A Preventive strategy method for voltage and reactive power dispatch", *IEEE Trans. on PAS*, vol. 104, no. 7, July 1985, pp. 1607-1676.

[35] C. W. Taylor, "*Power System Voltage Stability*", McGraw-Hill Inc., New York 1994.

[36] G. K. Morrison, B. Gao and P. Kundur, "Voltage stability analysis using static and dynamic approaches", *IEEE Trans. on PAS*, vol. 8, no. 3, August 1993, pp. 1159-1171.

[37] V. Ajjarapu, C. Christy, "The continuation power flow: A tool for steady state voltage stability analysis", *IEEE Trans. on PAS*, vol. 7, no. 1, February 1992. pp. 416-423.

[38] Power Tech. Labs Inc., "*VSTAB Users Manual*", January 1995.

[39] V. A. Venikov, V. I. Stroes, V. I. Idelchuk and V. I. Tarasov, "Estimation of electric power system steady state stability in load flow calculations", *IEEE Trans. on PAS*, vol. 94, no. 3, May-June 1975, pp. 1034-1038.

[40] K. P. Kessel and H. Glavitsch, "Estimating the voltage stability of a power System ", *IEEE Trans. on Power Delivery*, vol. PWRD-1, no.3, July 1986, pp. 346-354.

Appendix A

Optimal Power Flow Program

A.1 Main Module

This appendix gives the details about the Optimal Power Flow (OPF) program and the files required to run the OPF problem. The main module of the OPF program was coded using C++ language. This program reads the data from four different files, namely line data file, bus data file, generator data file and problem definition file. The main module is executed to formulate the OPF problem in a format which can be solved by using the general purpose software MINOS. The details of the input files are given below:

A.2 Line data file

The Line data is stored in a file "line.dat". This file contains the information about the transmission lines in the system, information about the tap changing transformers and line ratings. The format of the file is given below:

columns $1-7$: *Line number*

columns $8-15$: *Bus number where the line starts*

columns $16-23$: *Bus number where the line ends*

columns $24-31$: *Information about tap changer*

0 – *No tap changers*

1 – *Tap changers present*

columns $32-39$: *Branch resistance* R_s *(per unit)*

columns $40-47$: *Branch reactance* X_s *(per unit)*

columns $48-55$: *Branch shunt conductance* G_s *(per unit)*

columns $56-63$: *Branch shunt susceptance* B *(per unit)*

columns $64-71$: *Minimum tap settings*

columns $72-79$: *Maximum tap settings*

columns $80-88$: *Maximum line MVA rating*

A.3 Bus data file

The Bus data is stored in a file "bus.dat". This file contains the information about the bus type, bus voltages, generation at the bus and the load at various buses. The details of the file are given below

columns $1-7$: *Bus number*

columns $8-15$: *Bus type*

1 – *Slack or reference bus*

2 – *Generator bus*

3 – *Load bus*

columns $16-23$: *Minimum Bus voltage*

columns $24-31$: *Maximum Bus voltage*

columns $32-39$: *Minimum real power generation* (MW)

columns $40-47$: *Maximum real power generation* (MW)

columns $48-55$: *Load* (MW)

columns $56-63$: *Load* $(MVAR)$

columns $64-71$: *Mimimum reactive power generation* $(MVAR)$

columns $72-79$: *Maximum reactive power generation* $(MVAR)$

A.4 Generator data file

The generator data is stored in a file "gen.dat". This file contains the information about the generator cost coefficients and shunt capacitors available at various buses. The details of the file are given below

columns $1-7$: *Bus number*

columns $8-15$: *Generator information*

0 – *No Generator at the Bus*

1 – *Generator present at the Bus*

columns $16-23$: *No information (type zero in this column)*

columns $24-31$: *Capacitor and generator information*

0 – *No Generator at the bus*

2 – *Generator present at the bus*

2 – *Capacitor banks present at the bus*

columns $32-39$: *Generator cost coefficient* (α)

columns $40-47$: *Generator cost coefficient* (β)

columns $48-55$: *Generator cost coefficient* (γ)

columns $56-63$: *Minimum value of capacitor* ($MVAR$)

columns $64-71$: *Maximum value of capacitor* ($MVAR$)

A.5 Problem definition file

This file is stored in a file "prob.dat". This file contains the parameters used to define the OPF problem. The format of the file is shown below:

Number of buses in the system

xx

Number of Lines in the system

xx

Number of Generators in the system

xx

Number of Tap changers in the system

xx

Number of capacitor banks in the system

xx

Number of line with contains shunt capacitors

xx

Table A.1: OPF input data files for various test systems

	Line data file	Bus data file	Generator data file	Problem definition file	Initialization file
6 Bus system	b6l.dat	b6b.dat	b6g.dat	prob6.dat	ini6.dat
14 Bus system	b14l.dat	b14b.dat	b14g.dat	prob14.dat	ini14.dat
30 Bus system	b30l.dat	b30b.dat	b30g.dat	prob30.dat	ini30.dat

A.6 Sample data files

Sample data files for the line, bus, generator and problem definition files for the 6 Bus system, IEEE 14 bus system and Modified IEEE 30 bus system are stored in the directory in kilo machine under the directory /usr/local/minos/opf96. The available sample data file names for the three test system are summarized in the Table A.1.

A.7 Optimization process

The optimization is carried out by a general purpose software called MINOS. MINOS requires three standard input files namely "*.f", "*.mps" and "*.spc". The details of these files are discussed in the MINOS users manual [25]. The main C-program formulates the OPF problem in the form of these standard files and the MINOS optimization routine is used to solve the OPF problem. All the files needed to execute the MINOS are stored in the directory /usr/local/minos/opf96.

A.8 Running the OPF problem

This section gives the various commands needed to formulate and run the OPF problem. The entire process is done by the following two commands:

% opf

This command runs the main C program (opf.c) module and reads the data from the input files namely "line.dat", "bus.dat", "gen.dat" and "prob.dat". The OPF problem is formulated in three standard files namely "op.f", "op.mps" and "op.spc" as required by MINOS.

% opfmin

This command runs the optimization routine in MINOS and solves the OPF problem and the results of the optimization are stored in the file "op.out".

A.9 Output file

The results of the optimization are stored in a file called "op.out". This file stores the optimization results in a standard format as given in the MINOS user manual. This section explains how to interpret the results from this output file.

The important results of the OPF problem are the value of the objective function and the values of the state and control variables. The value of the objective function can be easily read from the output file. The values of the state and control variables are stored in an array of variable X. The value of state and control variable can be determined from this variables with the help of problem definition file. For example if the test system contains :

n : *number of buses*

g : *number of generators*

t : *number of tap changing transformers*

c : *number of variable capacitors banks*

pv : *number of voltage control buses*

The total array size of X will be (2n+2g+t+c). The variables of the array X will represent the following state and control variable.

$$X(1) - X(n) \quad : \quad \textit{the bus voltage magnitude at the buses}$$

$$X(n+1) - X(2n) \quad : \quad \textit{the bus voltage angles at the buses}$$

$$X(2n+1) - X(2n+g) \quad : \quad \textit{the real power generation at various generator buses}$$

$$X(2n+g+1) - X(2n+2g) \quad : \quad \textit{the reactive power generation at various generator buses}$$

$$X(2n+2g+1) - X(2n+2g+t) \quad : \quad \textit{the value of tap setting for the tap changing transformers}$$

$$X(2n+2g+t+1) - X(2n+2g+t+c) \quad : \quad \textit{the value of capacitors at the capacitor b}$$

where

$$(2n+2g+t+c) \quad : \quad \textit{is the total number of state variables}$$

$$(pv+(g-1)+t+c) \quad : \quad \textit{is the total number of control variables}$$

A.10 Example

This section explains how to run the OPF problem using the available test systems. In this discussion the OPF problem is simulated for the 6 bus system. The 6 bus system files namely "b6l.dat", "b6b.dat", "b6g.dat" and "prob6.dat" are copied to the standard input files namely "line.dat", "bus.dat", "gen.dat" and "prob.dat". The command *opf* is used to formulated the OPF problem in the standard MINOS

format. The command *opfmin* is used to solve the optimization process using MINOS. The result is stored in the file "op.out". All input files used to solve the OPF problem for a 6 bus system and the output file (results) are attached to this Appendix.

Input data files for 6 Bus system

line.dat

1	1	6	1	0.123	0.518	0	0.04	0.9	1.1	1.0
2	1	4	0	0.080	0.370	0	0.028	0	0	1.0
3	4	6	0	0.097	0.407	0	0.03	0	0	1.0
4	6	5	1	0.000	0.286	0	0	0.9	1.1	1.0
5	5	2	0	0.282	0.640	0	0	0	0	1.0
6	2	3	0	0.723	1.050	0	0	0	0	1.0
7	3	4	1	0.000	0.110	0	0	0.9	1.1	1.0

bus.dat

1	3	1.00	1.10	0	1.2	0	0	-.20	1.0
2	2	1.00	1.10	0	0.5	0	0	-.20	1.0
3	1	0.95	1.05	0	0	.55	.13	0	0
4	1	0.95	1.05	0	0	0	0	0	0
5	1	0.95	1.05	0	0	.3	.18	0	0
6	1	0.95	1.05	0	0	.5	.05	0	0

gen.dat

1	1	0	1	0	1	.05	0	0
2	1	0	1	0	1	.01	0	0
3	0	0	0	0	0	0	0	0
4	0	0	2	0	0	0	0	0.165
5	0	0	0	0	0	0	0	0
6	0	0	2	0	0	0	0	0.175

Prob.dat

```
Bus
6
Line
7
Generators
2
Tap_settings
3
Static_vars
2
Equ_line_num
0
```

The OPF results for the 6 Bus system

op.out

```
      ******************************
      M I N O S    5.4    (Dec 1992)
      ******************************

    Begin            Optimal_power_flow
    Problem Number           1
    Nonlinear Variables      21              <------   total no. of variables
    Nonlinear Constraints    27              <------   total no. of constraints
    Jacobian                 Dense
    Rows                     77
    Columns                  71
    Elements                 10934
    Print level                    0
    MPS file                 10
    Derivative level         0
    Major Iterations         200
    End              Optimal_power_flow

Reasonable Workspace limits are         0 ...   87372
Actual     Workspace limits are         0 ... 2000000 ... 2000000  words of  z.
1

MPS file
--------
     1    *-->&lt;------>  &lt;------>  &lt;---------->   &lt;------>  &lt;---------->
     2    NAME          Optimal_power_flow
     3    ROWS
    31    COLUMNS
XXXX  Warning - no linear objective selected
    53    RHS
    81    BOUNDS
   145    ENDATA


Names selected
--------------
Objective               (Min)        0
RHS             RHS                 27
RANGES                               0
BOUNDS          BOUND               42


No. of Jacobian entries specified          0
No. of LAGRANGE entries specified          0
No. of INITIAL  bounds  specified          21
No. of superbasics specified               21

Nonzeros allowed for in LU factors    998243
Scale option  0,      Partial price        1
Partial price section size (A)             21
Partial price section size (I)             27


Matrix Statistics
-----------------
              Total       Normal         Free       Fixed     Bounded
Rows             27            7            0          20           0
Columns          21            0            0           1          20

No. of matrix elements                    567     Density     100.000
Biggest                          0.0000E+00  (excluding fixed columns,
Smallest                         0.0000E+00   free rows, and RHS)

No. of objective coefficients              0


Number of Nonlinear constraints           27
Number of Linear    constraints            0
Number of Variables                       21
1

Initial basis
```

```
------------

No basis file supplied


funcon  sets       0   out of     567   constraint gradients.


funobj  sets       0   out of      21   objective  gradients.


Crash option  3
1

Iterations
----------

Major minor   total ninf  sinf/objective    viol    rg    nsb    ncon xchange lchange    step     LU penalty
    0     0       0    0 0.00000000E+00 4.5E-01 0.0E+00   21      23 0.0E+00 0.0E+00 1.0E+00      0 1.0E+00
    1    0T       0    0 0.00000000E+00 4.5E-01 0.0E+00   21      23 0.0E+00 0.0E+00 1.0E+00     27 1.0E+00
Crash on nonlinear rows:
Slacks     7  Free cols     0  Preferred     0
Unit       0  Double        0  Triangle      0  Pad    20
    2    23      23    0 5.48670884E+02 1.4E-01 0.0E+00    0     167 1.3E-01 5.9E+03 1.0E+00    109 1.0E+00
Search exit  5 -- step too small.       Itn =     32   Norm rg =  4.522E+00
    3     9      32    0 5.90974458E+02 7.0E-02 4.5E+00    3     439 7.9E-02 1.3E-01 1.0E+00     97 1.0E+00
    4     3      35    0 6.00947308E+02 1.8E-03 2.4E-01    3     513 9.0E-03 7.0E-03 1.0E+00     90 1.0E+00
    5     2      37    0 6.01257122E+02 1.5E-06 1.0E-03    3     583 3.7E-04 2.7E-04 1.0E+00     84 1.0E-01
    6     1      38    0 6.01257278E+02 3.3E-11 1.5E-04    3     630 9.1E-07 2.2E-07 1.0E+00     84 1.0E-02
1

EXIT -- optimal solution found

power_fl                              ---------------------------------------
No. of iterations                38   | Objective value      6.0125727842E+02 |
                                      ---------------------------------------

No. of major iterations             6   Linear objective      0.0000000000E+00
Penalty parameter            0.001000   Nonlinear objective  6.0125727842E+02
No. of calls to funobj            629   No. of calls to funcon            630
Calls with mode=2 (f, known g)     26   Calls with mode=2 (f, known g)     28
Calls for forward differencing    546   Calls for forward differencing    546
Calls for central differencing      0   Calls for central differencing      0
No. of superbasics                  3   Norm of reduced gradient     1.469E-04
No. of basic nonlinears            12   Norm rg / Norm pi            1.188E-07
No. of degenerate steps             0   Percentage                        0.00
Norm of x                   2.025E+00   Norm of pi                   1.236E+03
Primal infeas            0    0.0E+00   Dual infeas               6    1.5E-04
Constraint violation        3.289E-11   Normalized                   1.087E-11
1


NAME          power_fl             OBJECTIVE VALUE       6.0125727842E+02
                                                         ----------------
                                    ( Total operating cost )


STATUS        OPTIMAL SOLN         ITERATION     38    SUPERBASICS     3

OBJECTIVE               (Min)
RHS           RHS
RANGES
BOUNDS        BOUND

SECTION 1 - ROWS

 NUMBER  ...ROW.. STATE  ...ACTIVITY...  SLACK ACTIVITY  ..LOWER LIMIT.  ..UPPER LIMIT.  .DUAL ACTIVITY    ..I

     22  CON1         EQ        0.00000         0.00000         0.00000         0.00000     -1030.78400      1
     23  CON2         EQ        0.00000         0.00000         0.00000         0.00000      -914.24984      2
     24  CON3         EQ        0.00000         0.00000         0.00000         0.00000     -1112.15682      3
     25  CON4         EQ        0.00000         0.00000         0.00000         0.00000     -1107.96194      4
     26  CON5         EQ        0.00000         0.00000         0.00000         0.00000     -1109.35546      5
     27  CON6         EQ        0.00000         0.00000         0.00000         0.00000     -1120.25141      6
     28  CON7      A  EQ        0.00000         0.00000         0.00000         0.00000         0.00000      7
```

29	CON8	A	EQ	0.00000	0.00000	0.00000	0.00000	0.00000	8
30	CON9		EQ	0.00000	0.00000	0.00000	0.00000	-0.17182	9
31	CON10	A	EQ	0.00000	0.00000	0.00000	0.00000	0.00000	10
32	CON11		EQ	0.00000	0.00000	0.00000	0.00000	-15.13544	11
33	CON12		EQ	0.00000	0.00000	0.00000	0.00000	-13.63232	12

CON13 to CON19 ---> MVA flows in the lines

				MVA flows (in p.u)					
34	CON13		BS	0.46467	0.53533	NONE	1.00000	0.00000	13
35	CON14		BS	0.49077	0.50923	NONE	1.00000	0.00000	14
36	CON15		BS	0.08154	0.91846	NONE	1.00000	0.00000	15
37	CON16		BS	0.20551	0.79449	NONE	1.00000	0.00000	16
38	CON17		BS	0.29506	0.70494	NONE	1.00000	0.00000	17
39	CON18		BS	0.18183	0.81817	NONE	1.00000	0.00000	18
40	CON19		BS	0.42531	0.57469	NONE	1.00000	0.00000	19
41	CON20	D	BS	0.00000	0.00000	0.00000	0.00000	0.00000	20
42	CON21	D	BS	0.00000	0.00000	0.00000	0.00000	0.00000	21
43	CON22	D	BS	0.00000	0.00000	0.00000	0.00000	0.00000	22
44	CON23	D	BS	0.00000	0.00000	0.00000	0.00000	0.00000	23
45	CON24	D	BS	0.00000	0.00000	0.00000	0.00000	0.00000	24
46	CON25	D	BS	0.00000	0.00000	0.00000	0.00000	0.00000	25
47	CON26	D	BS	0.00000	0.00000	0.00000	0.00000	0.00000	26
48	CON27	D	BS	0.00000	0.00000	0.00000	0.00000	0.00000	27

1

SECTION 2 - COLUMNS

NUMBER	.COLUMN.	STATE	...ACTIVITY...	.OBJ GRADIENT.	..LOWER LIMIT.	..UPPER LIMIT.	REDUCED GRADNT	M+J
	X1 - X6	------->	Bus voltages magnitudes (p.u)					
			V (p.u)					
1	X1	UL	1.10000	0.00000	1.00000	1.10000	-4.88593	28
2	X2	UL	1.10000	0.00000	1.00000	1.10000	-89.58320	29
3	X3	SBS	1.01120	0.00000	0.95000	1.05000	-0.00007	30
4	X4	UL	1.05000	0.00000	0.95000	1.05000	-75.28379	31
5	X5	SBS	1.0104e	0.00000	0.95000	1.05000	0.00003	32
6	X6	SBS	1.04935	0.00000	0.95000	1.05000	0.00015	33
	X7 - X12	------->	Bus voltage angles (p.u)					
			Delta (p.u)					
7	X7	EQ	0.00000	0.00000	0.00000	0.00000	0.00390	34
8	X8	BS	-0.0082?	0.00000	-2.00000	2.00000	0.00000	35
9	X9	BS	-0.1897?	0.00000	-2.00000	2.00000	0.00000	36
10	X10	BS	-0.1502?	0.00000	-2.00000	2.00000	0.00000	37
11	X11	BS	-0.18261	0.00000	-2.00000	2.00000	0.00000	38
12	X12	BS	-0.18120	0.00000	-2.00000	2.00000	0.00000	39
	X13 - X14	------->	Real power generation (p.u)					
			PG (p.u)					
13	X13	BS	0.93078	1030.78400	0.00000	1.20000	0.00000	40
14	X14	UL	0.50000	200.00008	0.00000	0.50000	-714.24976	41
	X15 - X17	------->	Tap settings of the transformers.					
15	X15	BS	0.96574	0.00000	0.90000	1.10000	0.00000	42
16	X16	BS	0.9847?	0.00000	0.90000	1.10000	0.00000	43
17	X17	BS	0.98108	0.00000	0.90000	1.10000	0.00000	44
	X18 - X19	------->	Reactive power generation (p.u)					
			QG (p.u)					

```
    18  x18          BS          0.16689          0.00000         -0.20000          1.00000          0.00000      45
    19  x19          BS          0.02537          0.00000         -0.20000          1.00000          0.00000      46

       x20 - x21      ------>    static capacitance (p.u)

    20  x20          BS          0.12547          0.00000          0.00000          0.16500          0.00000      47
    21  x21          UL          0.17500          0.00000          0.00000          0.17500        -15.01101      48

funcon called with nstate =   2

funobj called with nstate =   2

Time for MPS input                              0.09 seconds
Time for solving problem                        0.35 seconds
Time for solution output                        0.04 seconds
Time for constraint functions                   0.11 seconds
Time for objective function                     0.03 seconds
Endrun
```

Appendix B

OPF System Data

This appendix gives the various line, bus and generator data required for the OPF problem. This appendix includes the data for the three different test systems namely the 6-bus system, IEEE 14-bus system and IEEE 30-bus system.

Table B.1: Line data for the 6-Bus system

Branch No.	Bus No.'s	R p.u	X p.u	B(total) p.u	Rating MVA
1	1-6	0.123	0.518	0.040	100
2	1-4	0.080	0.370	0.028	100
3	4-6	0.097	0.407	0.030	100
4	6-5	0.000	0.286	0.000	100
5	5-2	0.282	0.640	0.000	100
6	2-3	0.723	1.050	0.000	100
7	3-4	0.000	0.110	0.000	100

Table B.2: Bus data for the 6-Bus system

Bus No.	Load P MW	Load Q MVAR
1	0	0
2	0	0
3	55	13
4	0	0
5	30	18
6	50	5

Table B.3: Generator data for the 6-Bus system

Bus No.	P_G^{min} MW	P_G^{max} MW	Q_G^{min} MVAR	Q_G^{max} MVAR	a	b	c
1	10	100	-20	100	0	1.00	0.05
2	10	100	-10	100	0	1.00	0.01

Table B.4: Line data for the IEEE-14 Bus system

Branch No.	Bus No.'s	R p.u	X p.u	B(total) p.u	Rating MVA
1	1-2	0.01938	0.05917	0.0528	200
2	1-5	0.05403	0.22304	0.0492	200
3	2-3	0.04699	0.19797	0.0438	200
4	2-4	0.05811	0.17632	0.0374	200
5	2-5	0.05695	0.17388	0.0340	200
6	3-4	0.06701	0.17103	0.0340	200
7	4-5	0.01335	0.04211	0.0128	200
8	4-7	0.00000	0.20912	0.0000	200
9	9-4	0.00000	0.55618	0.0000	200
10	5-6	0.00000	0.25202	0.0000	200
11	6-11	0.09498	0.19890	0.0000	200
12	6-12	0.12291	0.25581	0.0000	200
13	6-13	0.06615	0.13027	0.0000	200
14	7-8	0.00000	0.17615	0.0000	200
15	7-9	0.00000	0.11001	0.0000	200
16	9-10	0.03181	0.08450	0.0000	200
17	9-14	0.12711	0.27038	0.0000	200
18	10-11	0.08205	0.19207	0.0000	200
19	12-13	0.22092	0.19988	0.0000	200
20	13-14	0.17093	0.34802	0.0000	200

Table B.5: Bus data for the IEEE-14 Bus system

Bus No.	Load P MW	Load Q MVAR
1	0	0
2	21.7	12.7
3	94.2	19.0
4	47.8	-3.9
5	27.6	11.6
6	11.2	7.5
7	0	0
8	0	0
9	20.5	10.6
10	20.0	10.8
11	20.5	10.8
12	20.1	10.6
13	10.5	5.8
14	10.9	5.0

Table B.6: Generator data for the IEEE-14 Bus system

Bus No.	P_G^{min} MW	P_G^{max} MW	Q_G^{min} MVAR	Q_G^{max} MVAR	a	b	c
1	0	340	-50	200	0	2.25	0.0083
2	0	70	-40	50	0	1.00	0.0625
3	0	80	0	40	0	1.75	0.0175
6	0	90	0	50	0	3.00	0.0250
8	0	70	0	50	0	3.00	0.0260

Table B.7: Line data for the 30-Bus system

Branch No.	Bus No.'s	R p.u	X p.u	B(total) p.u	Rating MVA
1	1-2	0.0192	0.0575	0.0528	130
2	1-3	0.0452	0.1852	0.0408	130
3	2-4	0.0570	0.1737	0.0368	65
4	3-4	0.0132	0.0379	0.0084	130
5	2-5	0.0472	0.1983	0.0418	130
6	2-6	0.0581	0.1763	0.0374	65
7	4-6	0.0119	0.0414	0.0090	90
8	5-7	0.0460	0.1160	0.0204	70
9	6-7	0.0267	0.0820	0.0170	130
10	6-8	0.0120	0.0420	0.0090	32
11	6-9	0.0000	0.2080	0.0000	65
12	10-6	0.0000	0.5560	0.0000	32
13	9-11	0.0000	0.2080	0.0000	65
14	9-10	0.0000	0.1100	0.0000	65
15	4-12	0.0000	0.2560	0.0000	65
16	12-13	0.0000	0.1400	0.0000	65
17	12-14	0.1231	0.2559	0.0000	32
18	12-15	0.0662	0.1304	0.0000	32
19	12-16	0.0945	0.1987	0.0000	32
20	14-15	0.2210	0.1997	0.0000	16
21	16-17	0.0824	0.1932	0.0000	16
22	15-18	0.1070	0.2185	0.0000	16
23	18-19	0.0639	0.1292	0.0000	16
24	19-20	0.0340	0.0680	0.0000	32
25	10-20	0.0936	0.2090	0.0000	32
26	10-17	0.0324	0.0845	0.0000	32
27	10-21	0.0348	0.0749	0.0000	32
28	10-22	0.0727	0.1499	0.0000	32
29	21-22	0.0116	0.0236	0.0000	32
32	23-24	0.1320	0.2700	0.0000	16
33	24-25	0.1885	0.3292	0.0000	16
34	25-26	0.2544	0.3800	0.0000	16
35	25-27	0.1093	0.2087	0.0000	16
36	28-27	0.0000	0.3960	0.0000	65
37	27-29	0.2198	0.4153	0.0000	16
38	27-30	0.3202	0.6027	0.0000	16
39	29-30	0.2399	0.4533	0.0000	16
40	8-28	0.0636	0.2000	0.0428	32
41	6-28	0.0169	0.0599	0.0130	32
42	10-10	0.0000	5.26		
43	24-24	0.0000	25.0		

Table B.8: Bus data for the 30-Bus system

Bus No.	Load P MW	Load Q MVAR
1	0	0
2	21.7	12.7
3	2.4	1.2
4	7.6	1.6
5	94.2	19.0
6	0	0
7	22.8	10.9
8	30.0	30.0
9	0	0
10	5.8	2.0
11	0	0
12	11.2	7.5
13	0	0
14	6.2	1.6
15	8.2	2.5
16	3.5	1.8
17	9.0	5.8
18	3.2	0.9
19	9.5	3.4
20	2.2	0.7
21	17.5	11.2
22	0	0
23	3.2	1.6
24	8.7	6.7
25	0	0
26	3.5	2.3
27	0	0
28	0	0
29	2.4	0.9
30	10.6	1.9

Table B.9: Generator data for the 30-Bus system

Bus No.	P_G^{min} MW	P_G^{max} MW	Q_G^{min} MVAR	Q_G^{max} MVAR	a	b	c
1	50	200	-20	250	0	2.00	0.0037
2	20	80	-20	100	0	1.75	0.0175
5	15	50	-15	80	0	1.00	0.0625
8	10	35	-15	60	0	3.25	0.0083
11	10	30	-10	50	0	3.00	0.0250
13	12	40	-15	60	0	3.00	0.0250